Controllable Donor–Acceptor Neutral [2]Rotaxanes

Takahiro Iijima,[a] Scott A. Vignon,[a] Hsian-Rong Tseng,[a] Thibaut Jarrosson,[b] Jeremy K. M. Sanders,*[b] Filippo Marchioni,[c] Margherita Venturi,*[c] Emanuela Apostoli,[c] Vincenzo Balzani,[c] and J. Fraser Stoddart*[a]

Abstract: In pursuit of a neutral bistable [2]rotaxane made up of two tetraarylmethane stoppers—both carrying one isopropyl and two *tert*-butyl groups located at the *para* positions on each of three of the four aryl rings—known to permit the slippage of the π-electron-donating 1,5-dinaphtho[38]crown-10 (1/5DNP38C10) at the thermodynamic instigation of π-electron-accepting recognition sites, in this case, pyromellitic diimide (PmI) and 1,4,5,8-naphthalenetetracarboxylate diimide (NpI) units separated from each other along the rod section of the rotaxane's dumbbell component, and from the *para* positions of the fourth aryl group of the two stoppers by pentamethylene chains, a modular approach was employed in the synthesis of the dumbbell-shaped compound **NpPmD**, as well as of its two degenerate counterparts, one (**PmPmD**) which contains two PmI units and the other (**NpNpD**) which contains two NpI units. The bistable [2]rotaxane **NpPmR**, as well as its two degenerate analogues **PmPmR** and **NpNpR**, were obtained from the corresponding dumbbell-shaped compounds **NpPmD**, **PmPmD**, and **NpNpD** and 1/5DNP38C10 by slippage. Dynamic ^{1}H NMR spectroscopy in CD_2Cl_2 revealed that shuttling of the 1/5DNP38C10 ring occurs in **NpNpR** and **PmPmR**, with activation barriers of 277 K of 14.0 and 10.9 kcal mol^{-1}, respectively, reflecting a much more pronounced donor–acceptor stabilizing interaction involving the NpI units over the PmI ones. The photophysical and electrochemical properties of the three neutral [2]rotaxanes and their dumbbell-shaped precursors have also been investigated in CH_2Cl_2. Interactions between 1/5DNP38C10 and PmI and NpI units located within the rod section of the dumbbell components of the [2]rotaxane give rise to the appearance of charge-transfer bands, the energies of which correlate with the electron-accepting properties of the two diimide moieties. Comparison between the positions of the visible absorption bands in the three [2]rotaxanes shows that, in **NpPmR**, the major translational isomer is the one in which 1/5DNP38C10 encircles the NpI unit. Correlations of the reduction potentials for all the compounds studied confirm that, in this non-degenerate [2]rotaxane, one of the translational isomers predominates. Furthermore, after deactivation of the NpI unit by one-electron reduction, the 1/5DNP38C10 macrocycle moves to the PmI unit. Li^+ ions have been found to strengthen the interaction between the electron-donating crown ether and the electron-accepting diimide units, particularly the PmI one. Titration experiments show that two Li^+ ions are involved in the strengthening of the donor–acceptor interaction. Addition of Li^+ ions to **NpPmR** induces the 1/5DNP38C10 macrocycle to move from the NpI to the PmI unit. The Li^+-ion-promoted switching of **NpPmR** in a 4:1 mixture of CD_2Cl_2 and CD_3COCD_3 has also been shown by ^{1}H NMR spectroscopy to involve the mechanical movement of the 1/5DNP38C10 macrocycle from the NpI to the PmI unit, a process that can be reversed by adding an excess of [12]crown-4 to sequester the Li^+ ions.

Keywords: bistable switches · molecular devices · rotaxanes · self-assembly · template synthesis

[a] T. Iijima, S. A. Vignon, Dr. H.-R. Tseng, Prof. J. F. Stoddart
California NanoSystems Institute and
Department of Chemistry and Biochemistry
University of California, Los Angeles
405 Hilgard Avenue, Los Angeles, CA 90095-1569 (USA)
Fax: (+1) 310-206-1843
E-mail: stoddart@chem.ucla.edu

[b] T. Jarrosson, Prof. J. K. M. Sanders
Cambridge Center for Molecular Recognition
University Chemical Laboratory
Lensfield Road, Cambridge CB2 1EW (UK)
Fax: (+44) 122-333-6362
E-mail: jkms@cam.ac.uk

[c] F. Marchioni, Prof. M. Venturi, E. Apostoli, Prof. V. Balzani
Dipartimento di Chimica "G. Ciamician"
Università di Bologna
Via Selmi 2, 40126 Bologna (Italy)
Fax: (+39) 051-209-9456
E-mail: margherita.venturi@unibo.it

 DOI: 10.1002/chem.200400651

Introduction

During the past decade, supramolecular chemistry[1] has provided synthetic chemists with a powerful methodology in the form of template-directed protocols[2] to construct molecular-scale machines.[3,4] The opportunity to incorporate wholly synthetic motor molecules, as the active components during the engineering of nanoelectromechanical systems[5] and in the fabrication of nanoelectronic devices,[6] makes it feasible to consider a bottom-up approach for the miniaturization of devices. Some of us at UCLA have helped to realize molecular-switch tunnel junctions (MSTJs)[6c] based on a series of amphiphilic, bistable [2]rotaxanes,[7] in which a tetracationic ring component, cyclobis(paraquat-*p*-phenylene) ($CBPQT^{4+}$), is located around a neutral dumbbell component, containing two recognition sites—a tetrathiafulvalene (TTF) unit and a 1,5-dioxynaphthalene (DNP) ring system—for the cyclophane situated some way apart from each other within the central polyether section of the dumbbell, which is terminated by a hydrophobic stopper at one end and by a hydrophilic stopper at the other. Although the amphiphilic character of these bistable [2]rotaxanes allows them to be self-organized[6c,8] at the air–water interface in a Langmuir trough, before being transferred as uniform monolayers into the MSTJs of functioning devices, there is some evidence[7] from electrochemical experiments carried out by some of us in Bologna, supported by ^{1}H NMR spectroscopic data obtained at UCLA, that some of these (amphiphilic) bistable [2]rotaxanes adopt folded conformations in solution (Figure 1). Also, since the thicknesses of the Langmuir–Blodgett (LB) monolayers are always considerably less than might be predicted on the basis of essentially linear amphiphiles, it is not unlikely that some of the solution-state, structural features of the molecules will be present, even in compressed films at the air–water interface. Indeed, there is some circumstantial evidence[9] from in-depth studies of amphiphilic, bistable [2]rotaxanes with a variety of constitutionally different (more and less) hydrophilic tails, that 1) the thinner than expected LB films, 2) the observed footprints in the first liquid-condensed and second highly condensed phases, and 3) their area differential, all compared as a function of the constitution of the hydrophilic tails, are consistent with the presence in the Langmuir films of an equilibrium (Figure 2) between folded and unfolded conformations. Moreover, the pressure–area isotherm data are consistent with a model in which, as the hydrophilicities of the rotaxanes' tails or the surface pressure of the Langmuir films are increased, the equilibria lie closer to the unfolded conformations.

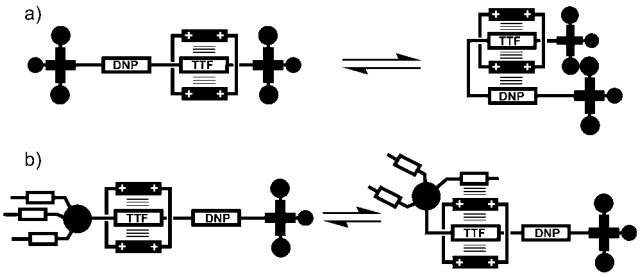

Figure 1. Schematic representations of a) the equilibrium between the folded/unfolded conformations of a bistable [2]rotaxane in solution and b) the equilibrium between possible folding/unfolding conformations of the amphiphilic, bistable [2]rotaxane in solution. The π-electronic donating unit associated with hydrophilic stopper folds back to form an alongside π–π stacking interaction with the $CPBQT^{4+}$ ring.

Notwithstanding all the potential problems associated with the self-organization of these positively charged, amphiphilic [2]rotaxanes at the air–water interface and their transfer employing the LB technique, MSTJs have been fabricated[6c,8] by sandwiching self-organized monolayers of the amphiphilic, bistable [2]rotaxanes between bottom polysilicon electrodes and top electrodes of titanium covered with aluminum. The devices have been shown[6c] to exhibit hysteretic current–voltage responses on account of marked differences in conductance[10] between the ground (low) state, when the $CBPQT^{4+}$ ring encircles the TTF unit, and the metastable (high) state, when the $CBPQT^{4+}$ ring encircles the DNP ring systems, of a range of amphiphilic, bistable [2]rotaxanes.[7] However, the tetracationic nature of the $CBPQT^{4+}$ ring component may introduce complications during the LB stage of the device fabrication (Figure 2) or the supporting counterions, which are supplied as four hexafluorophosphate anions (PF_6^-), may exercise some profound influence during the electromechanical switching processes[11] that involve the mechanical movement of the $CBPQT^{4+}$ ring between the ground and the metastable states, that is, the OFF and ON states of the switch, respec-

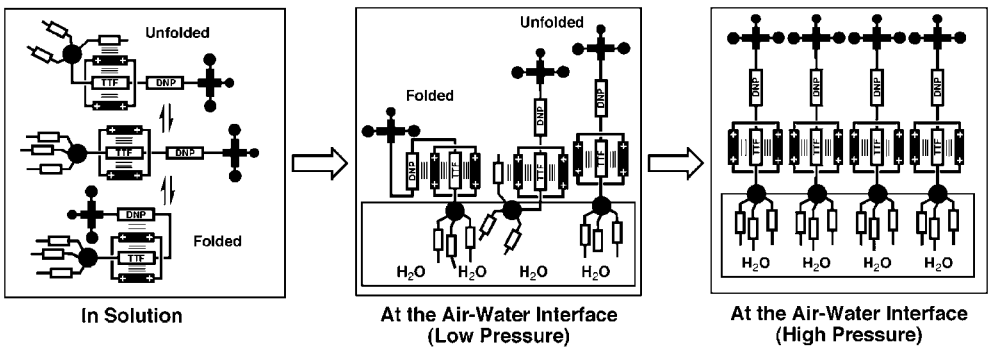

Figure 2. Some of the possible conformational equilibria and self-organization behaviors displayed by an amphiphilic, bistable [2]rotaxane in solution (left), in low-pressure condensed phases (middle), and in high-pressure condensed phases (right).

tively. The evident question arises: what do the ions, PF_6^- or otherwise, do in the molecular monolayer of the solid-state device (Figure 3) during the electromechanical movement of the $CBPQT^{4+}$ ring? Do they follow it, thus conferring drag upon the movement of the ring, for example? The answer to this question is that we do not know and so would like to be better informed on these fundamental issues pertaining to molecular electronic devices containing positively charged bistable [2]rotaxane molecules.

During the past few years, some of us in Cambridge (England) have pioneered[12] a donor–acceptor recognition system based on neutral π-electron-accepting sites, as well as neutral π-electron-donating sites, for the efficient assembly of neutral catenanes and rotaxanes using template-directed synthesis.[2] With reference to [2]rotaxanes,[12i,k] the neutral π-electron-rich aromatic crown ether, namely 1,5-dinaphtho[38]crown-10 (1/5DNP38C10), has been located around the neutral π-electron-accepting 1,4,5,8-naphthalenetetracarboxylic diimide[13] (NpI) unit. With the ultimate objective of realizing neutral [2]rotaxanes of high bistabilities (and moderate metastability) that can be switched by controlling the redox properties of the molecules, we have identified pyromellitic diimide[14] (PmI) as a much weaker recognition site to compete with an NpI site for encirclement by a 1/5DNP38C10 macrocycle around the dumbbell-shaped component of a [2]rotaxane. We would anticipate that π–π stacking and other weak noncovalent interactions involving the 1/5DNP38C10 macrocycle encircling the stronger (NpI) of the two π-electron-accepting recognition sites would result in these [2]rotaxanes existing essentially as one translational isomer,[15] with the weaker (PmI) site to all intents and purposes unpopulated by the 1/5DNP38C10 macrocycle. Another requirement of this particular design of a neutral molecular switch is that it can be thrown electromechanically between two different states. Since the reduction potential of a bare NpI unit is considerably lower[16] than that for a bare PmI unit, the opportunity does exist to control (Figure 4) the switching of such a bistable [2]rotaxane with redox chemistry.

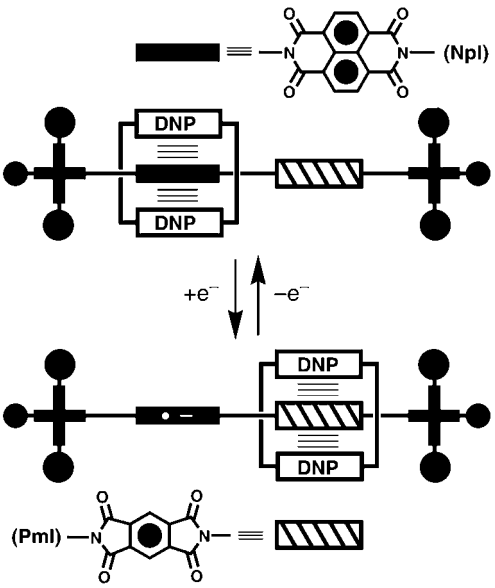

Figure 4. A schematic representation of redox switching in a bistable [2]rotaxane.

After satisfying this requirement, the next challenge becomes one of being able to synthesize the potentially bistable [2]rotaxane **NpPmR**, shown in Figure 5a, along with its degenerate counterparts **NpNpR** and **PmPmR** illustrated in Figure 5b and c, respectively. In general, template-directed protocols[2] have been applied to the synthesis of two-station [2]rotaxanes in which the reliance is placed upon either kinetic or thermodynamic control,[17] with the latter able to involve dynamic covalent chemistry,[18] as well as supramolecular (noncovalent) synthesis, for example, slippage.[19] Although a number of different thermodynamic synthetic approaches are being pursued actively at UCLA and in Cambridge, the research reported in this paper employs slippage as the final step in the syntheses of the three [2]rotaxanes **NpPmR**, **NpNpR**, and **PmPmR** from their corresponding

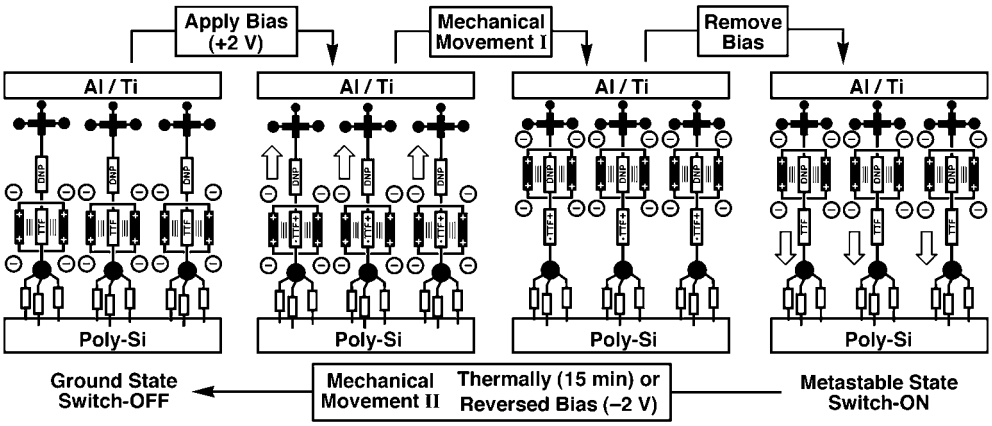

Figure 3. Proposed electromechanical mechanism which accounts for the hysteretic current–voltage response by an amphiphilic, bistable [2]rotaxane monolayer in an MSTJ device. The devices which are described in reference [6c] consist of rotaxane molecules with 1) an amphiphilic dumbbell component containing two recognition sites (a TTF unit and a DNP ring system) and two stoppers (one (upper) hydrophobic and the other (lower) hydrophilic); and 2) a macrocycle, the tetracationic cyclophane, cyclobis(paraquat-*p*-phenylene), accompanied by four hexafluorophosphate anions (PF_6^-, ⊖), See reference [6c] for the structural formulas of rotaxanes that give hysteretic current–voltage responses in device settings. Note that the graphical representations of the amphiphilic bistable [2]rotaxane molecules are highly idealized.

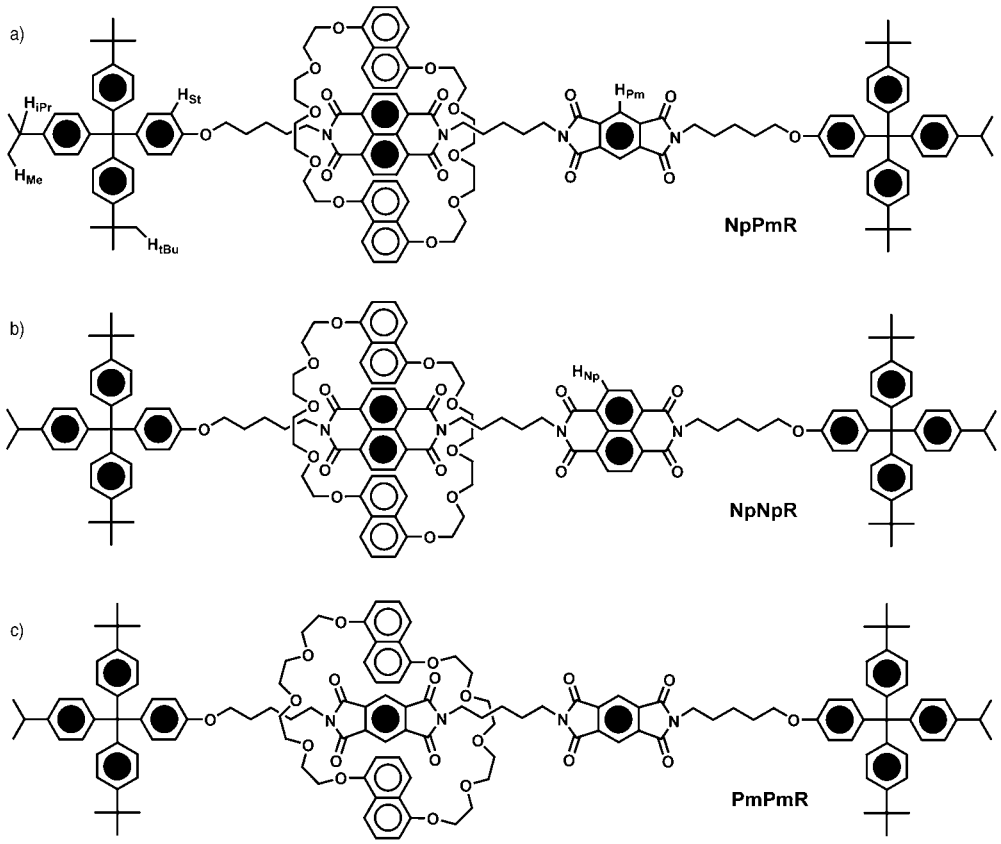

Figure 5. Structural formulas for the a) bistable [2]rotaxane **NpPmR** and the degenerate [2]rotaxanes b) **NpNpR**, and c) **PmPmR**.

dumbbell-shaped compounds **NpPmD**, **NpNpD**, and **PmPmD**; hence, the choice of the tetraarylmethane stoppers[20] carrying two *tert*-butyl groups and one isopropyl group which are known[21] to permit the passage of 1/5DNP38C10 macrocycles in solution at slightly elevated temperatures with respect to those normally found in a research laboratory.

In this paper, we describe 1) the synthesis of two degenerate model [2]rotaxanes **PmPmR** and **NpNpR** and a non-degenerate, bistable [2]rotaxane **NpPmR**; 2) their characterization by mass spectrometry, by (dynamic) NMR and UV-visible spectroscopy, and by electrochemistry; and 3) the switching of **NpPmR** by chemical (Li^+ ions) as well as electrochemical means.

Results and Discussion

Design and synthetic strategy: Retrosynthetic analyses of the degenerate [2]rotaxanes **PmPmR** and **NpNpR** and the nondegenerate [2]rotaxane **NpPmR** suggested to us a limited number of viable synthetic pathways. Common to all of the pathways was the slippage procedure,[19] which we decided to employ to incorporate 1/5DNP38C10 around the dumbbell-shaped compounds, that is, it constitutes the last step of all three syntheses summarized in Schemes 1–3. In the syntheses of the dumbbell-shaped compounds **PmPmD**, **NpNpD**, and **NpPmD**, a modular approach was adopted to assemble progressively the four fragments, namely 1) two tetraarylmethane stoppers[11] suitable for the slippage of 1/5DNP38C10 and 2) the PmI and/or NpI recognition sites, separated by pentamethylene chains. Moreover, the reactions chosen (Schemes 1–3) for connecting each fragment were nucleophilic substitution reactions carried out under Mitsunobu reaction conditions.

Synthesis: The routes employed in the syntheses of two degenerate neutral, two-station [2]rotaxanes are outlined in Scheme 1 and 2. The preparation of the dumbbell-shaped compound **PmPmD** (Scheme 1) began with the alkylation of the tetraarylmethane stopper **1**[20] by 5-chloro-1-pentanol in MeCN in the presence of LiBr and [18]crown-6 (18C6) as catalysts, and K_2CO_3 as the base. Following flash column chromatography, the alcohol **2** was obtained in 83%. Using Mitsunobu reaction conditions (PPh_3/diethylazodicarboxylate (DEAD)), pyromellitic diimide (**3**) was reacted with the alcohol **2** and the mono-THP-protected 1,5-pentandiol **4**.[22] Without purification, the product was converted into the half-dumbbell compound **5** by HCl-catalyzed deprotection in wet CH_2Cl_2 with an overall yield of 37%. The synthesis of the dumbbell-shaped compound **PmPmD** was accomplished in 33% yield, once again by using Mitsunobu reaction conditions (PPh_3/DEAD) on a mixture of compound **5**, the alcohol **2**, and pyromellitic diimide (**3**) in THF. The [2]rotaxane **PmPmR** was obtained by a template-assisted slippage protocol, wherein the dumbbell-shaped compound **PmPmD** served as the template. Compound **PmPmD** was treated with an excess of the macrocycle 1/5DNP38C10

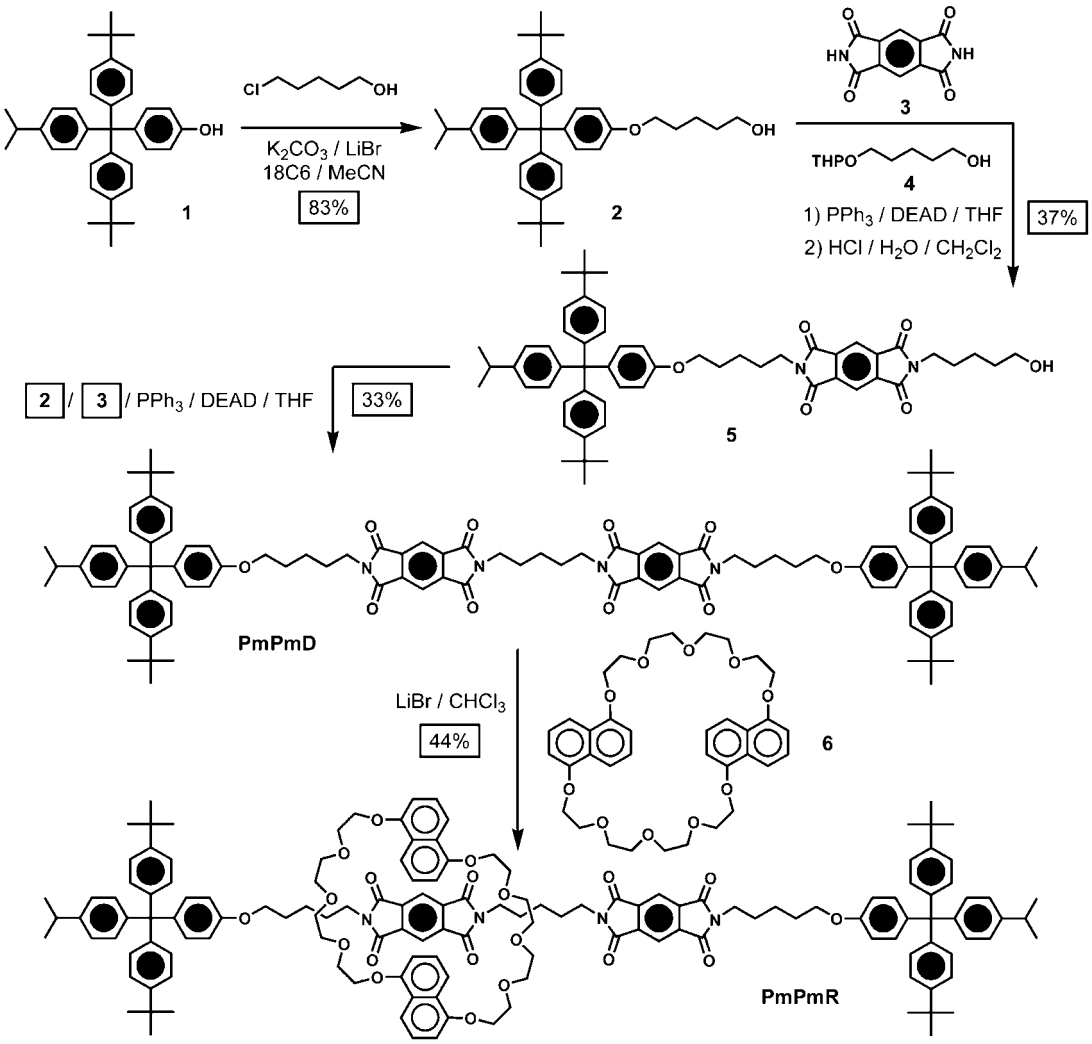

Scheme 1. Synthesis of the PmI-containing degenerate [2]rotaxane **PmPmR** and its dumbbell-shaped precursor **PmPmD**.

(**6**)[23] in the presence of LiBr in a $CHCl_3$/MeOH (95:5) solvent mixture at 60 °C for 14 days. After column chromatography, the [2]rotaxane **PmPmR** was obtained in a yield of 44 % as an analytically pure yellow solid.

The sequence of steps employed in the synthesis of dumbbell-shaped compound **NpNpD** and degenerate rotaxane **NpNpR** is summarized in Scheme 2. The half-dumbbell compound **8** was obtained in an overall yield of 33 % by alkylating naphthalene diimide (**7**) with the alcohol **2** and the mono-THP-protected 1,5-pentanediol **4**[22] by using Mitsunobu reaction conditions (PPh_3/DEAD), followed by HCl-catalyzed deprotection in CH_2Cl_2. The synthesis of the dumbbell-shaped compound **NpNpD** was accomplished in 40 % yield after another Mitsunobu reaction carried out on compound **8**, the alcohol **2**, and naphthalene diimide (**7**)[24] in THF. The template-directed synthesis of the [2]rotaxane **NpNpR** proceeded in 42 % yield when a mixture of the dumbbell-shaped compound **NpNpD**, the macrocycle 1/5DNP38C10 (**6**)[22] and LiBr is in a $CHCl_3$/MeOH solvent mixture, employing exactly the same reaction and purification conditions as those described for the preparation of rotaxane **NpNpR**.

The template-directed synthesis of the nondegenerate [2]rotaxane **NpPmR** from its dumbbell-shaped precursor **NpPmR** is summarized in Scheme 3. The synthesis of the dumbbell **NpPmD** was accomplished in 30 % yield by carrying out a Mitsunobu reaction (PPh_3/DEAD) between the half-dumbbell compound **5**, the alcohol **2**, and naphthalene diimide (**7**) in THF. The template-directed synthesis of the [2]rotaxane **NpPmR** proceeded in 52 % yield when a mixture of the dumbbell-shaped compound **NpPmD**, the macrocycle 1/5DNP38C10 (**6**)[23] and LiBr were reacted in a $CHCl_3$/MeOH solvent mixture, by using exactly the same reaction and purification conditions as those described for the preparation of [2]rotaxanes **NpNpR** and **PmPmR**.

Mass spectrometric investigation: The mass spectrometric data for the dumbbell-shaped compounds **NpNpD**, **PmPmD**, and **NpPmD**, and for the [2]rotaxanes **NpNpR**, **PmPmR**, and **NpPmR** are summarized in Table 1. All of these compounds were characterized by matrix-assisted laser-desorption ionization time-of-flight (MALDI-TOF) mass spectrometry. The positively-charged ions $[M+Na]^+$ or $[M+H]^+$ were observed in their mass spectra.

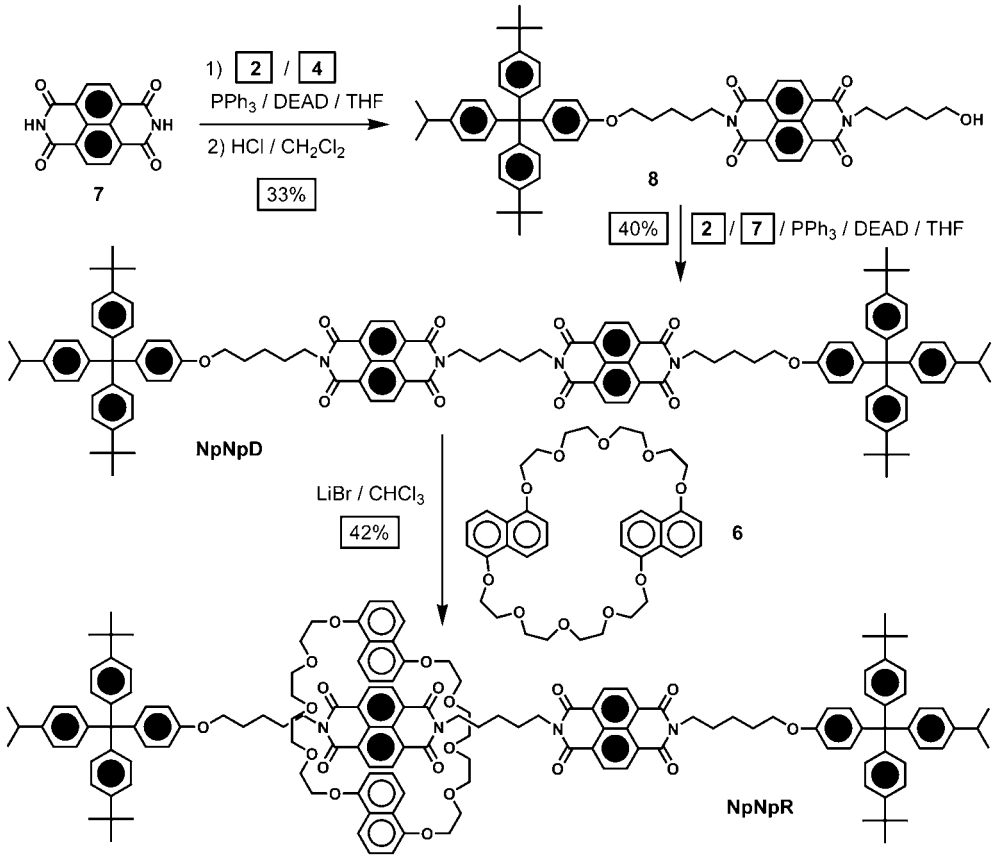

Scheme 2. Synthesis of the NpI-containing degenerate [2]rotaxane **NpNpR** and its dumbbell-shaped precursor **NpNpD**.

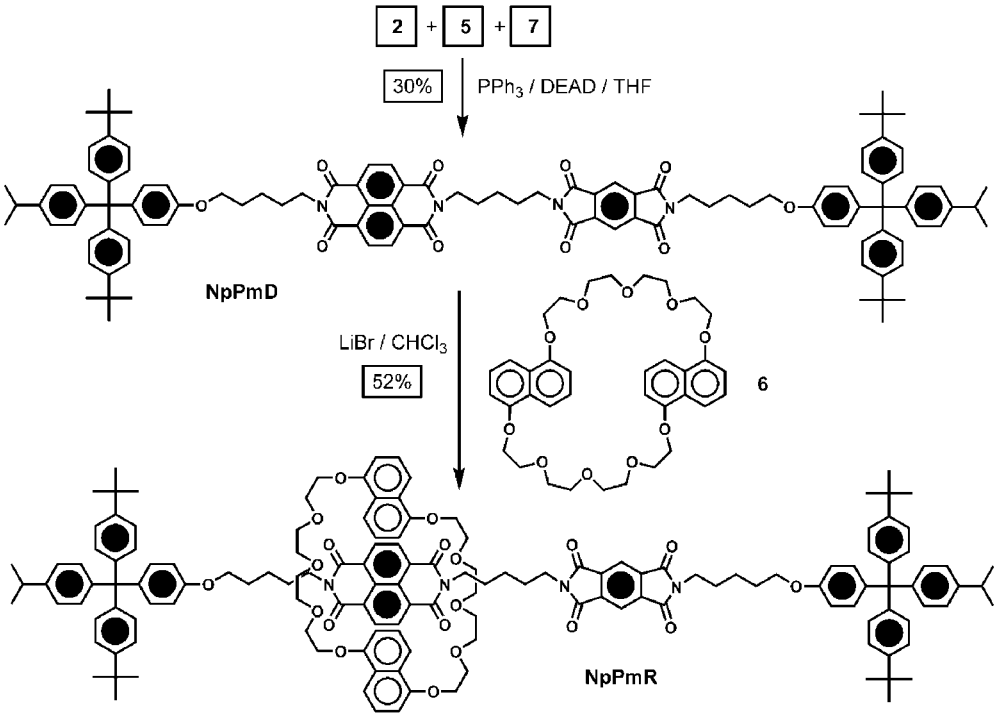

Scheme 3. Synthesis of the bistable [2]rotaxane **NpPmR** containing both NpI and PmI units and its dumbbell-shaped precursor **NpPmD**.

(Dynamic) ^{1}H NMR spectroscopic study: We have employed variable-temperature ^{1}H NMR spectroscopy to probe the kinetics and thermodynamics of the shuttling processes[26] (Figure 6) in the two degenerate rotaxanes, **PmPmR** and **NpNpR**. At low temperatures, the shuttling processes are slow on the ^{1}H NMR timescale and the signals, shown in Table 2, separate out into two equal intensity sets of signals. As the temperature is increased, the shuttling

Table 1. MALDI-TOF MS data for the dumbbell-shaped compounds **NpNpD**, **PmPmD** and **NpPmD**, and for the [2]rotaxanes **NpNpR**, **PmPmR** and **NpPmR**.

	NpNpD	**PmPmD**	**NpPmD**	**NpNpR**	**PmPmR**	**NpPmR**
ion	$[M+Na]^+$	$[M+H]^+$	$[M+Na]^+$	$[M+Na]^+$	$[M+Na]^+$	$[M+H]^+$
m/z	1640	1718	1690	2277	2377	2304

process becomes fast on the ^{1}H NMR timescale and averaged signals are observed. Table 2 gives low- and high-temperature chemical shifts in CD_2Cl_2 for a few sample probe protons for each degenerate rotaxane. In order to study the dynamics of shuttling, one set of probe protons for each rotaxane was chosen. The aromatic protons on the hydrophobic stopper, which give rise to the signals centered on $\delta =$ 6.75 and 6.83 ppm were chosen as the probes for **NpNpR**, while the resonances for the protons of the PmI unit appearing at $\delta = 6.96$ and 8.32 ppm were used for **PmPmR**. These δ values were obtained from spectra recorded in CD_2Cl_2 at 209 K. Rate constants were then determined at different temperatures for these shuttling processes by simulating the partial spectra (see Figure 7 for the simulations of **NpNpR**) by using Spinworks 2.1[27] and matching them as closely as possible with the experimentally observed spectra. The kinetic and derived thermodynamic data are listed in Tables 3 and 4. From a comparison of $\Delta G^{\neq}$ values recorded in these two tables, it is evident that **NpNpR** [for which $\Delta G^{\neq}$ ranges from 13.9 (at 305 K) to 14.1 kcal mol^{-1} (at 266 K)], containing the stronger electron-accepting NpI units, presents a considerably larger barrier (3.1 kcal mol^{-1} at 277 K) for the shuttling of the 1/5DNP38C10 macrocycle relative to that

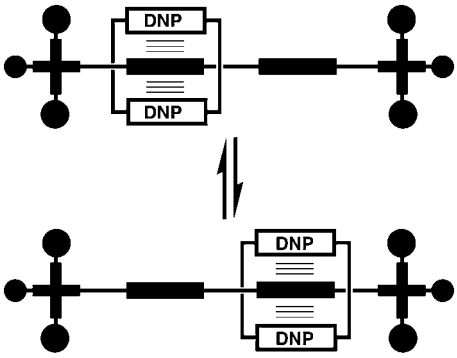

Figure 6. A graphical representation of the shuttling process in a degenerate [2]rotaxane with two identical stations.

Table 2. ^{1}H NMR chemical shift values for select protons of the degenerate shuttles at high and low temperature in CD_2Cl_2 at 600 MHz.

	Assignment[a]	Limiting δ values (low temperature)	*T* [K]	Limiting δ values (high temperature)	*T* [K]
PmPmR	H_{Pm}	6.96 (br), 8.32 (br)	209	7.67 (s)	319
	H_{St}	6.75 (d), 6.81 (d)	209	6.78 (d)	248
NpNpR	H_{Np}	8.21 (br), 8.80 (m)	248	8.52 (br)	332
	H_{St}	6.75 (d), 6.83 (d)	209	6.79 (d)	294
	H_{iPr}	2.85 (hp), 2.86 (hp)	209	2.87 (h)	277
	H_{tBu}	1.26 (s), 1.27 (s)	209	1.29 (s)	277

[a] Structural assignments for these protons can be found in Figure 5.

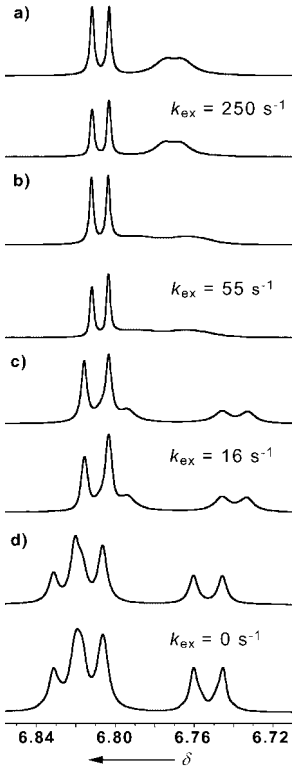

Figure 7. Simulated (top) and experimental (bottom) partial ^{1}H NMR spectra (600 MHz) recorded for **NpNpR** in CD_2Cl_2 at a) 294 K, b) 277 K, c) 266 K, and d) 226 K. The displayed region shows some of the resonances for the aromatic protons of the hydrophobic stopper (H_{St}, see Figure 5). The rate constants (k_{ex}) used to simulate the spectra are shown beside the spectra.

Table 3. Kinetic and thermodynamic data[a] for shuttling in **PmPmR** in CD_2Cl_2.

T [K][b]	k_{ex} [s^{-1}][c]	$\Delta G^{\neq}$ [kcal mol^{-1}][d]
226	45	11.4
239	300	11.2
248	1050	11.0
277	14500	10.9
294	50000	10.9

[a] These data were obtained by simulating the signals for the protons of the PmI unit (H_{Pm}) at $\delta = 8.32$ and 6.96 ppm (209 K), which coalesce into a single peak at $\delta = 7.63$ ppm (266 K). [b] Calibrated using neat MeOH sample. [c] Measured using line-shape analysis method. [d] $\pm$ 0.2 kcal mol^{-1}.

Table 4. Kinetic and thermodynamic data[a] for shuttling in **NpNpR** in CD_2Cl_2.

T [K][b]	k_{ex} [s^{-1}][c]	$\Delta G^{\neq}$ [kcal mol^{-1}][d]
266	16	14.1
277	55	14.0
294	250	14.0
305	650	13.9

[a] These data were obtained by simulating the signals for the aromatic protons of the hydrophobic stopper (H_{St}) at $\delta = 6.83$ and 6.75 ppm (226 K), which coalesce into a single peak at $\delta = 6.79$ ppm (294 K). [b] Calibrated using neat MeOH sample. [c] Measured using line shape analysis method. [d] ± 0.2 kcal mol^{-1}.

observed in **PmPmR** [for which $\Delta G^{\ddagger}$ ranges from 10.9 (at 294 K) to 11.4 kcal mol^{-1} (at 226 K)], with its weaker electron-accepting PmI units.

In the case of the bistable [2]rotaxane, **NpPmR**, no shuttling is observed by dynamic ^{1}H NMR spectroscopy. The 1/5DNP38C10 macrocycle resides, to all intents and purposes, on the NpI unit, at least to within the limits of detection provided by variable-temperature ^{1}H NMR spectroscopy. This heavily biased situation is evident from comparing the spectra presented in Figure 8. Signals for the protons (H_{Np}) on the NpI unit encircled by the macrocycle appear at $\delta = 8.13$ and 8.23 ppm (Figure 8c), while no signal is observed at $\delta \sim 8.8$ ppm where a resonance for the protons (H_{Np}) of the free NpI unit would be expected to appear (Figure 8a). Similarly, a signal for the protons (H_{Pm}) on the free PmI unit is observed at $\delta = 8.31$ ppm in the spectrum (Figure 8b) of **NpPmR**. No signal corresponding to an encircled PmI unit is observed in the region of $\delta =$ 6.9–7.0 ppm. From the difference (>3 kcal mol^{-1}) in the $\Delta G^{\ddagger}$ values (compare data in Tables 3 and 4) for shuttling in **PmPmR** and **NpNpR**, a rough estimate of the difference in binding energies of the NpI and PmI recognition sites would be ~ 3 kcal mol^{-1}. This prediction assumes that the difference in the free-energy barrier for shuttling in the two degenerate, two-station rotaxanes is dictated by ground-state interactions rather than transition-state ones. Whatever the rationalization, a free-energy difference between the two translational isomers of **NpPmR** of ~ 3 kcal mol^{-1} would mean that less than 1% of **NpPmR** resides in the translational isomer (not shown in Figure 5) in which the 1/5DNP38C10 macrocycle encircles the weaker electron-accepting PmI recognition site.

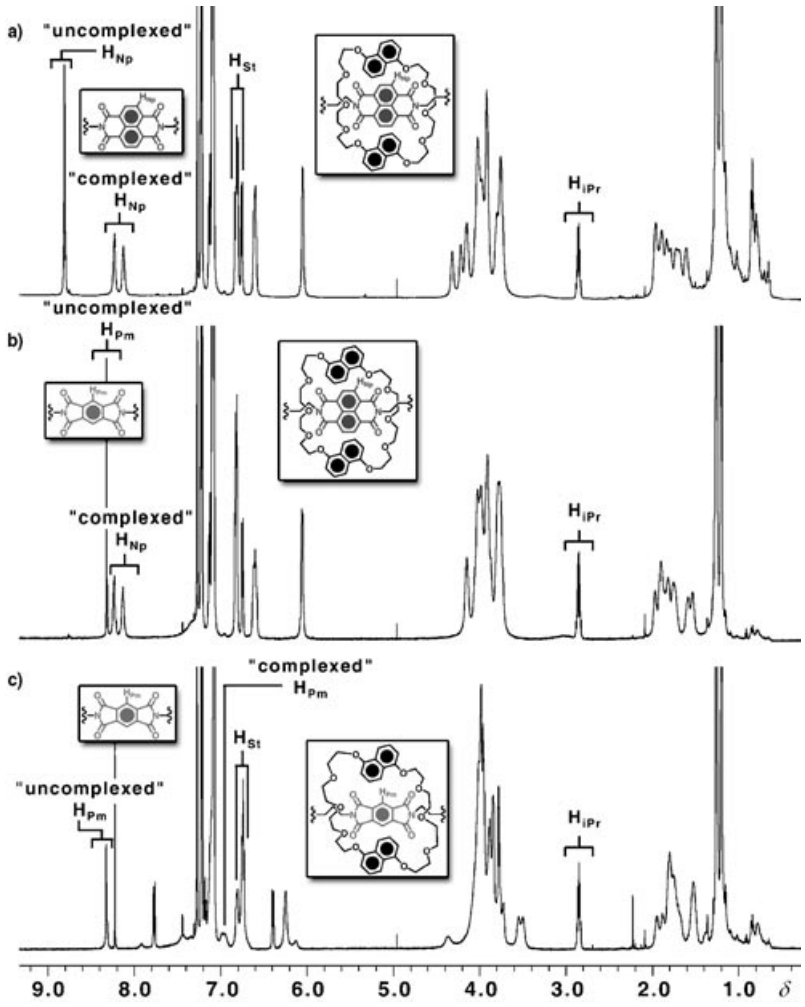

Figure 8. ^{1}H NMR Spectra (600 MHz) at room temperature in CD_2Cl_2 for a) **NpNpR**, b) **NpPmR**, and c) **PmPmR**. The insets show the partial structures for the three rotaxanes. Comparison of the spectrum for **NpPmR** with the two for the degenerate rotaxanes allows the observed signals to be assigned to the translational isomer where the ring resides on the NpI unit. The structural assignments for H_{iPr} and H_{St} can be found in Figure 5.

Yet another dynamic process can be observed in the two rotaxanes, **NpNpR** and **NpPmR**, which contain NpI units. As the temperature of the CD_2Cl_2 of these rotaxanes is lowered to 209 K, the signals corresponding to the protons of the NpI units, encircled by 1/5DNP38C10 macrocycles, separate (Figure 9) into multiple peaks. This behavior reflects a decrease in the local symmetry of the NpI unit, such that protons that were previously equivalent, on account of a particular site-exchange mechanism, are no longer equiva-

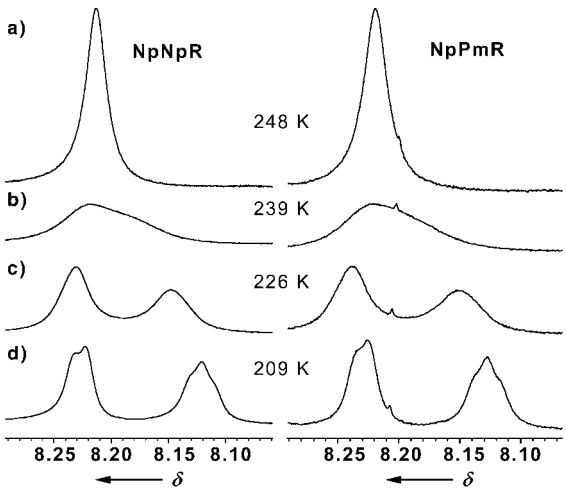

Figure 9. Partial ^{1}H NMR spectra (600 MHz) of **NpNpR** and **NpPmR**, recorded in CD_2Cl_2, showing the signals corresponding to the protons of the NpI unit, encircled by the 1/5DNP38C10 macrocycle, at a) 248 K, b) 239 K, c) 226 K, and d) 209 K.

lent on the ^{1}H NMR timescale. A diagram explaining the origin of this asymmetry is shown in Figure 10. In the absence of the macrocycle, the protons labeled H_a and H_c, as well as H_b and H_d, would be equivalent as a result of symmetry, both axial and planar symmetry relating them. However, the macrocycle does not share the same plane (and also axis most likely) of symmetry, possessing instead a C_2 axis, which is perpendicular to the plane of the NpI unit, resulting in all four protons being nonequivalent. A number of possible co-conformational changes could be proposed that would explain the site exchanges observed (Figure 10) for the two degenerate forms, but no clear evidence is available

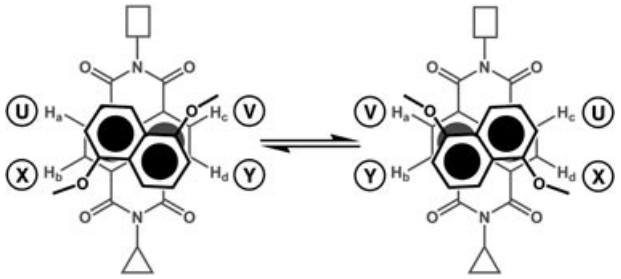

Figure 10. A schematic representation of the NpI unit encircled by a 1/5DNP38C10 macrocycle. If the indicated exchange process is slow on the ^{1}H NMR timescale, then all four protons would give rise to different signals in the spectrum, because the macrocycle does not share the plane of symmetry that would make H_a and H_c, as well as H_b and H_d, equivalent in the absence of the macrocycle. The squares and triangles represent the constitutionally distinct ends of the NpI unit in the rotaxane. H_a and H_c undergo exchange between sites U and V. H_b and H_d undergo exchange between sites X and Y.

to allow us to be precise at this time about the details of this mechanism. A rough estimate of the $\Delta G^{\neq}$ value for the exchange process can be made, based on the coalescence behaviors (Figure 9) of the signals, and gives a value of 11.5 kcal mol^{-1} at 239 K for both rotaxanes.[28] Similar processes have been observed previously in catenanes[29] and rotaxanes[30] containing 1,5-dioxynaphthalene units.

Photophysical investigations: The photophysical properties of all the compounds investigated were studied in air-equilibrated CH_2Cl_2 at room temperature. The [2]rotaxanes **PmPmR**, **NpNpR**, and **NpPmR** (Figure 5 and Schemes 1–3) contain four different types of chromophoric units, namely, the 1,5-dioxynaphthalene ring systems present in the 1/5DNP38C10 macrocycle and the tetraarylmethane stoppers as well as the PmI and/or NpI recognition sites present in the dumbbell components. We have also investigated model compounds related to the units contained in the dumbbell components, namely, the tetraarylmethane derivative **2** (Scheme 1) and the diimides **9** and **10**.

In CH_2Cl_2, 1/5DNP38C10 exhibits an absorption band with $\lambda_{max}=295$ nm, ($\varepsilon_{max}=16000\,M^{-1}\,cm^{-1}$) and a strong emission band (highest energy feature at 330 nm, $\Phi=0.10$, $\tau=7.6$ ns),[31] while the stopper precursor **2** shows absorption bands below 300 nm and a moderately intense ($\Phi=0.04$) and short-lived ($\tau=1.6$ ns) emission band with $\lambda_{max}=310$ nm

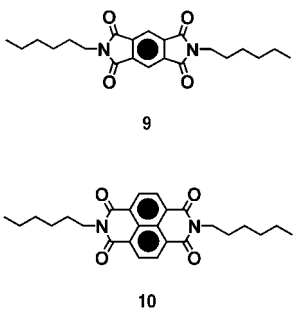

(Figure 11). The model compound **9** for the PmI recognition site shows a structured absorption band with $\lambda_{max}=320$ nm ($\varepsilon_{max}=2600\,M^{-1}\,cm^{-1}$) and no emission (Figure 12). The model compound **10** for the NpI recognition site exhibits

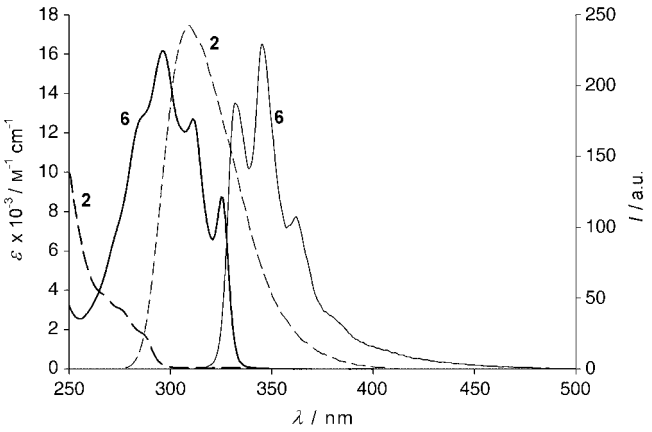

Figure 11. Absorption and emission spectra of the stopper precursor **2** and the crown ether **6** in air-equilibrated CH_2Cl_2 at room temperature.

a strongly structured band ($\lambda_{max}=380$ nm, $\varepsilon_{max}=26000\,M^{-1}\,cm^{-1}$), characteristic of its naphthalene core and a fluorescence band (highest energy feature at $\lambda_{max}=390$ nm, $\Phi=1.2\times10^{-3}$, $\tau<0.5$ ns), which is the mirror image of the absorption band (Figure 12). The data obtained for **9** and **10** are in agreement with previously reported results for compounds in the same family.[12a,32]

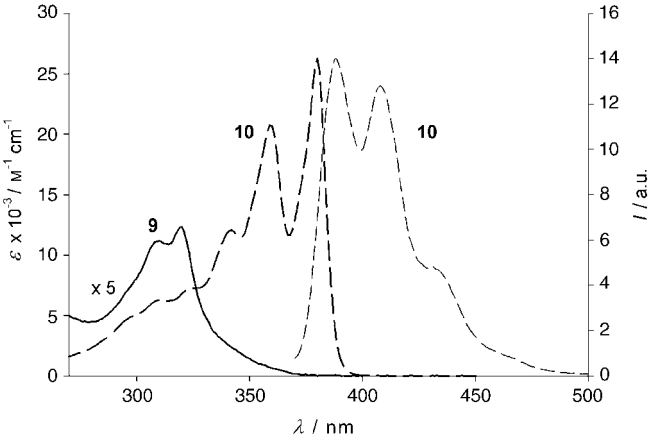

Figure 12. Absorption and emission spectra of model compounds **9** and **10** in air-equilibrated CH_2Cl_2 at room temperature.

The absorption spectra of the dumbbell compounds **PmPmD**, **NpNpD**, and **NpPmD** correspond to those expected from perusal of the spectra of the component units. As for the emission, however, the high-energy fluorescence of the stoppers is quenched, because of energy- and/or electron-transfer processes involving the diimide units, and the structured band of the NpI unit in **NpNpD** and **NpPmD** is partially quenched—presumably by a photoinduced electron-transfer process involving one of the stoppers—to about 50% of the intensity observed for model compound **10**.

The absorption spectra of the [2]rotaxanes **PmPmR**, **NpNpR**, and **NpPmR** differ considerably from what would have been expected on the basis of the spectra of their component units. It should be noted that there are strong differences in the spectral regions of both the ring component and diimide units. Furthermore, the strong decrease in the intensity of the UV region is accompanied (Figure 13) by the appearance of weak and broad absorption bands in the visible region. The presence of such low-energy excited states, a feature which is a generally observed for strong charge-transfer (CT) interactions, accounts for the lack of emission of the three [2]rotaxanes.[3d,4d,33]

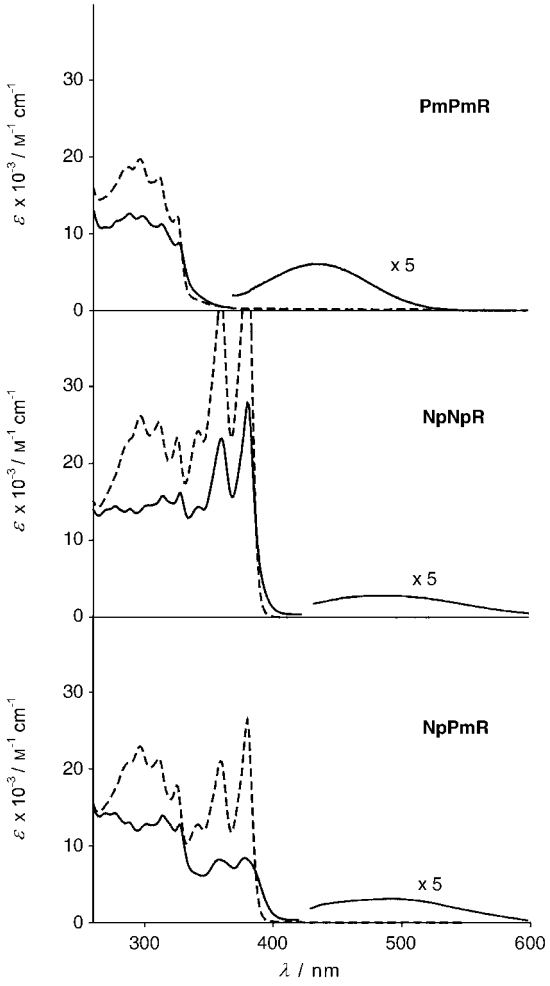

Figure 13. Absorption spectra in air-equilibrated CH_2Cl_2 at room temperature of the [2]rotaxanes **PmPmR**, **NpNpR**, and **NpPmR** (full lines) compared with the sums of the spectra of the component units (dashed lines).

We note that the maximum of the weak CT band in the visible region moves (Table 5) from 435 nm for **PmPmR** to 485 nm for **NpNpR**, a result that is consistent with the higher electron-accepting power of the NpI unit relative to that of the PmI one (see the section on electrochemical properties) and in agreement with the data previously obtained for related systems.[12g] We also note that the visible band for **NpPmR** is practically the same as that for **NpNpR**, an observation expected for the translational isomer of **NpPmR** in which the macrocycle encircles the NpI unit.

Table 5. Charge-transfer bands of the investigated compounds and complexes.[a]

	λ_{max} [nm]	ε [M^{-1} cm^{-1}]
PmPmR	435	1500
NpNpR	485	700
NpPmR	490	850
[**6**·**9**·Li_2]$^{2+}$	460	~350
[**6**·**10**·Li_2]$^{2+}$	550	~400
[**PmPmR**·Li_2]$^{2+}$	460	500
[**NpNpR**·Li_2]$^{2+}$	560	900
[**NpPmR**·Li_2]$^{2+}$	460	550

[a] In air-equilibrated CH_2Cl_2 at room temperature.

Electrochemical investigations and redox-induced switching of the bistable rotaxane: Electrochemical experiments—namely, cyclic voltammetry (CV) and differential pulse voltammetry (DPV)—were carried out in argon-purged CH_2Cl_2 solutions at room temperature. All the potential values are referred to SCE. Since the [2]rotaxanes **PmPmR**, **NpNpR**, and **NpPmR** all contain several electro-active units, they display a rather complex electrochemical behavior. We have focused our attention on the electrochemical behavior of the PmI and NpI recognition sites in order to understand, in the case of **NpPmR**, which site, if any, is surrounded preferentially by the macrocyclic ring and whether it is possible to induce ring shuttling by electrochemical stimulation.

Table 6 summarizes the results obtained. Both the model compounds **9** and **10** exhibit two monoelectronic and rever-

Table 6. Reduction processes of the PmI and NpI recognition sites contained in the **PmPmD**, **NpNpD**, **NpPmD** dumbbells, and in the **PmPmR**, **NpNpR**, **NpPmR** [2]rotaxanes, and in the model compounds **9** and **10**.[a]

	E^{I}_{NpI} [V][b]	E^{I}_{PmI} [V][b]	E^{II}_{NpI} [V][b]	E^{II}_{PmI} [V][b]
9		−0.89(1)		−1.42(1)
10	−0.65(1)		−1.05(1)	
PmPmD		−0.88(2)		−1.42(2)
NpNpD	−0.64(2)		−1.05(2)	
NpPmD	−0.65(1)	−0.90(1)	−1.05(1)	−1.45(1)
PmPmR		−0.87(1)		−1.43(2)
		−1.07(1)[c]		
NpNpR	−0.65(1)		−1.05(2)	
	−0.93(1)[c]			
NpPmR	−0.74(1)[c]	−1.06(1)[c,d]	−1.06(1)[d]	−1.47(1)

[a] Room temperature argon-purged CH_2Cl_2 solution; tetrabutylammonium hexafluorophosphate as the supporting electrolyte, glassy carbon as working electrode. [b] Potential value vs SCE; reversible process unless otherwise noted; number of the exchanged electrons reported in parentheses. [c] Process affected by a relatively slow heterogeneous electron-transfer rate. [d] For details, see the text.

sible reduction processes.[12g,34] The dumbbells **PmPmD** and **NpNpD**, which contain two PmI and NpI units, respectively, show bielectronic and reversible reduction processes at exactly the same potentials as observed for the corresponding model compounds (Figure 14), indicating that the two chemically and topologically equivalent units in each dumbbell behave independently. As expected, **NpPmD**, which contains both PmI and NpI recognition sites, shows four distinct, monoelectronic and reversible reduction processes for noninteracting units (Figure 14).

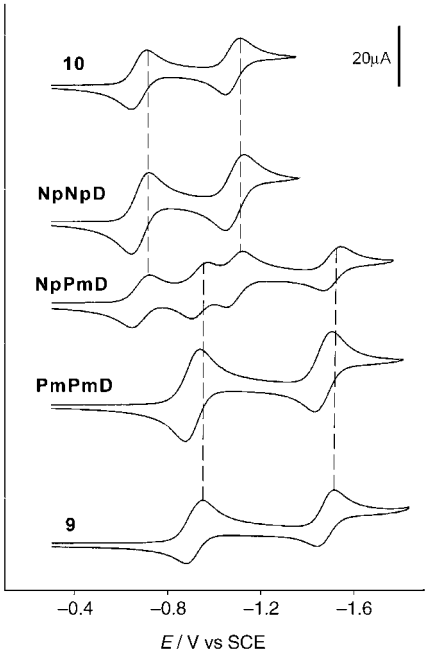

Figure 14. Cyclic voltammograms (argon-purged CH_2Cl_2; scan rate = 50 mVs^{-1}) of the dumbbells **PmPmD**, **NpNpD**, and **NpPmD** and of **9** and **10**, which serve as model compounds for the recognition sites. The CV waves have been corrected for different concentrations and diffusion coefficients.

The CV patterns for the reduction of the [2]rotaxanes **PmPmR**, **NpNpR**, and **NpPmR** are illustrated in Figure 15

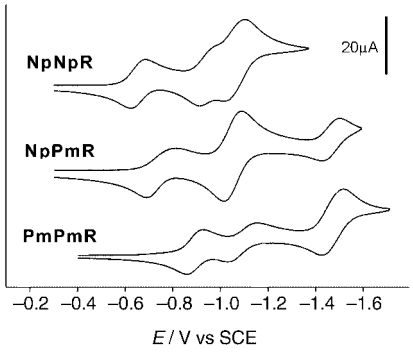

Figure 15. Cyclic voltammograms (argon-purged CH_2Cl_2; scan rate = 50 mVs^{-1}) of the [2]rotaxanes **PmPmR**, **NpNpR**, and **NpPmR**. The CV waves have been corrected for different concentrations and diffusion coefficients.

and the correlation diagram of the reduction potentials, observed in the dumbbell and rotaxane species, is presented in Figure 16. The results obtained indicate that, in the case of **PmPmR** and **NpNpR**, the two recognition sites are not equivalent. One unit is reduced at the same potential as in the corresponding dumbbell, whereas the second one is reduced at a more negative potential. This behavior demonstrates that, on the timescale of the heterogeneous electron-transfer process, the 1/5DNP38C10 macrocycle is localized on one of the two units. We also note that, in both [2]rotaxanes, the second reduction process of the two electron-accepting units takes place simultaneously and approximately at the same potential as the second reduction process observed in the corresponding dumbbell. This behavior establishes that there is no appreciable interaction between the macrocycle and the monoreduced PmI^- and NpI^- units.

In the case of the **NpPmR** rotaxane, which contains two different recognition sites, the first reduction process (−0.74 V) occurs (Table 6) at a potential more negative than that expected for a disengaged NpI unit—see the first reduction of the **NpNpD** and **NpPmD** dumbbells, and of the **NpNpR** rotaxane which occur at approximately −0.65 V. This result indicates clearly that the 1/5DNP38C10 macrocycle encircles the NpI recognition site. It is also evident that the second reduction wave of **NpPmR** is a two-electron process that occurs at a potential (−1.06 V) more negative than that of a disengaged PmI unit—see the first reduction of the **PmPmD** dumbbell and **PmPmR** rotaxane and the second reduction of the **NpPmD** dumbbell which both occur at about −0.90 V. This result demonstrates that, in **NpPmR**, the reduction of the NpI recognition site causes the displacement of the 1/5DNP38C10 macrocycle to the PmI unit. The shape of the CV curves as a function of sweep rate indicates that such a displacement is fast on the electrochemical timescale. As a consequence of the switching process, the monoreduced NpI^- unit is disengaged and is therefore expected to undergo second reduction at the same potential (−1.05 V) as in the dumbbell species. This sequence of events is consistent with the bielectronic nature of the second reduction wave at −1.06 V of **NpPmR** that can therefore be assigned to first reduction of engaged PmI and second reduction of disengaged NpI. The switching of the macrocycle from the one-electron reduced NpI^- to the PmI recognition site is confirmed by the fact that the first reduction of PmI occurs at the same potential (−1.07 V) as that of the second reduction process of **PmPmR**. The third reduction wave (−1.47 V) for **NpPmR** can be assigned quite straightforwardly to the reduction of a substantially disengaged PmI^- unit. When both the recognition sites are monoreduced, there is apparently no appreciable interaction with the macrocycle, just as in the cases of the degenerate **NpNpR** and **PmPmR** [2]rotaxanes.

It is also interesting to note that the reduction potential of the engaged NpI unit is more negative in **NpNpR** (−0.93 V) than in **NpPmR** (−0.74 V). This result can be accounted for by considering that, in the **NpPmR** rotaxane, reduction of the NpI unit is followed by a fast shuttling to the other (PmI) recognition site, whereas in the **NpNpR** rotaxane, reduction of the engaged NpI cannot be followed by

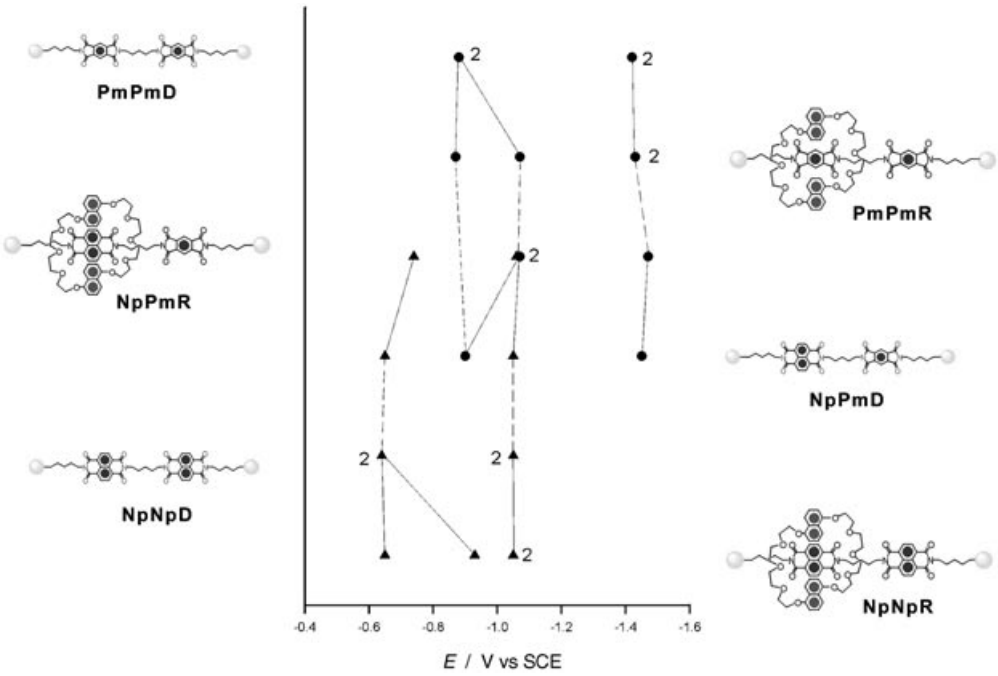

Figure 16. Correlations of the reduction potentials of the [2]rotaxanes **PmPmR**, **NpNpR**, and **NpPmR** with the dumbbells **PmPmD**, **NpNpD**, and **NpPmD**.

shuttling because the other recognition site has already been reduced as well.

Simulations of the CV patterns on the basis of the above discussed mechanism confirmed that shuttling is a fast process ($k > 105\ s^{-1}$) and showed that in all three [2]rotaxanes the reduction waves of the encircled units are not fully reversible, because of a slow heterogeneous electron transfer ($k < 0.02\ cm\ s^{-1}$). Such a behavior has already been observed for electroactive guests encapsulated in cage-like hosts, such as cyclodextrins, hemicarcerands, and dendrimers.[35]

Chemical switching of the bistable rotaxane: Previously, the interaction of Li^+ ions with PmI and NpI units and 1/5DNP38C10 (**6**) has been investigated.[36] Here, we report in more detail on the nature of these interactions. Addition of $LiClO_4$ (dissolved in MeCN) to a solution of **6** in CH_2Cl_2 causes small spectral changes in the absorption and emission bands of the macrocycle. No spectral change was observed when $LiClO_4$ was added to solutions of **9** or **10** in CH_2Cl_2. In CH_2Cl_2, association of either **9** or **10** with 1/5DNP38C10 (**6**) does not take place. When a solution containing equimolar amounts (8.0×10^{-5} M) of **6** and **9** or **10** was titrated by a solution of $LiClO_4$ in MeCN, strong spectral changes were observed—see, for example, Figure 17. Noticeably, a broad band with a maximum at 460 and 550 nm, respectively, was formed (Table 5), indicating that the presence of Li^+ ions promotes formation of a CT complex (presumably with a pseudorotaxane-like superstructure) between 1/5DNP38C10 and **9** or **10**. Titration plots (see the inset in Figure 17, for example) indicate that such complexes contain two Li^+ ions and exhibit high association constants. Some fuzziness in the isobestic points suggests that a 1:1 species is first formed, followed by formation of a 1:2 species. Titration of the $[\mathbf{6}\cdot\mathbf{10}\cdot Li_2]^{2+}$ complex with **9** causes (Table 5) a displacement of the visible band from 550 to 460 nm, demonstrating that the association constant of $[\mathbf{6}\cdot\mathbf{9}\cdot Li_2]^{2+}$ is larger than that of $[\mathbf{6}\cdot\mathbf{10}\cdot Li_2]^{2+}$.

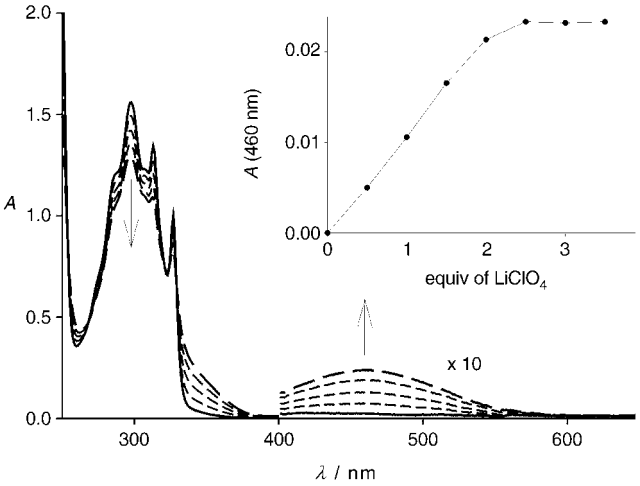

Figure 17. Spectral changes (optical path = 1 cm) observed upon titration of **9** and **6** (CH_2Cl_2, 8.0×10^{-5} M) with $LiClO_4$ (MeCN). The inset shows absorbance changes at 460 nm.

Titration of the degenerate **PmPmR** and **NpNpR** [2]rotaxanes with a solution of $LiClO_4$ in MeCN caused strong spectral changes to occur. As illustrated in Figure 18 for **PmPmR**, the CT band of the rotaxane ($\lambda_{max} = 435$ nm, Figure 14, Table 5) decreases in intensity and moves to the red, giving a band with $\lambda_{max} = 460$ nm, quite similar to that of the $[\mathbf{6}\cdot\mathbf{9}\cdot Li_2]^{2+}$ complex and reaching its maximum for addition of two equivalents of $LiClO_4$. In the same manner, addition of two equivalents of $LiClO_4$ to **NpNpR** causes the displacement of the CT band from 485 to 560 nm (Table 5). These results show clearly that the [2]rotaxanes are able to

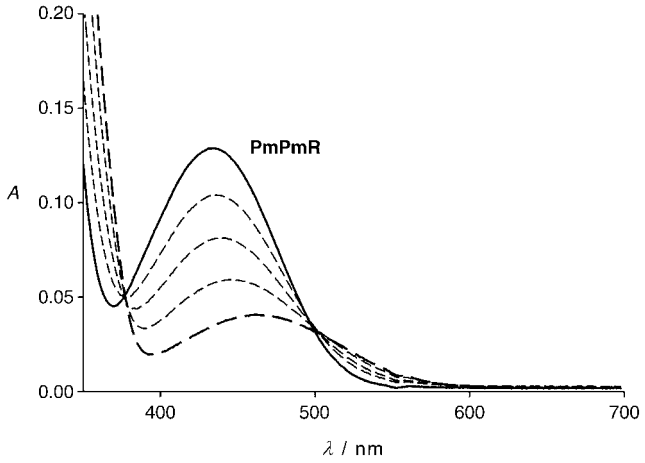

Figure 18. Spectral changes (optical path = 1 cm) observed upon titration of the degenerate **PmPmR** rotaxane (CH_2Cl_2, 8.0×10^{-5} M) with $LiClO_4$ (MeCN).

complex two Li^+ ions in order to form the $[\mathbf{PmPmR}\cdot Li_2]^{2+}$ and $[\mathbf{NpNpR}\cdot Li_2]^{2+}$ species. Since the presence of Li^+ affects the CT bands, we can also conclude that the metal ions are located close to the units involved in the donor–acceptor interactions.

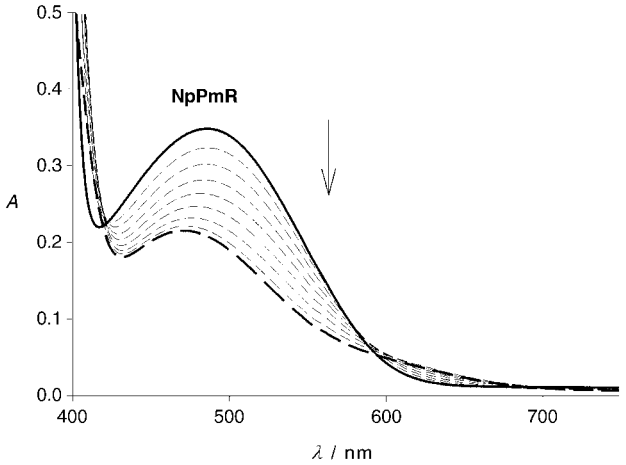

Figure 19. Spectral changes (optical path = 5 cm) observed upon titration of the nondegenerate **NpPmR** rotaxane (CH_2Cl_2, 8.0×10^{-5} M) with $LiClO_4$ (MeCN).

All the foregoing spectroscopic and electrochemical results indicate that, in the nondegenerate **NpPmR** rotaxane, the 1/5DNP38C10 macrocycle is located around the NpI station. However, the experiments performed on the pseudorotaxane-like species show that the presence of Li^+ ions favors formation of the $[\mathbf{6\cdot9}\cdot Li_2]^{2+}$ complex in preference to the $[\mathbf{6\cdot10}\cdot Li_2]^{2+}$ one. Taken together, these results suggest that addition of Li^+ ions to the **NpPmR** rotaxane should switch the 1/5DNP38C10 macrocycle from the NpI to the PmI recognition site. Such a switching is indeed observed, as indicated by the spectral changes displayed in Figure 19. They show that, upon addition of Li^+ ions, the CT band corresponding to the 1/5DNP38C10–NpI interaction is replaced by a CT band characteristic of the "Li^+-ion-assisted" 1/5DNP38C10–PmI interaction (Table 5).

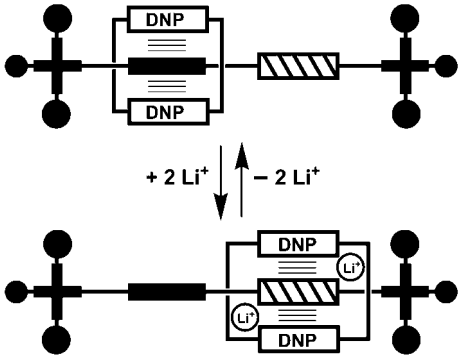

Figure 20. Schematic representation of the lithium-induced switching process of the bistable **NpPmR**. Addition of two equivalents of a lithium cation forms a complex between the crown ether, the PmI unit and two lithium cations that is stronger than the complex formed between the NpI unit and crown ether alone. Removal of the lithium cations disrupts this complex and causes the macrocycle to return to the stronger electron-accepting NpI unit.

We have also investigated the lithium-ion-induced switching process (Figure 20) in the bistable [2]rotaxane using ^1H NMR spectroscopy as the probe.[37] The spectrum of the neutral **NpPmR** at room temperature in CD_2Cl_2 is displayed in Figure 21a. This bistable [2]rotaxane exists predominately as the translational isomer (Figure 8) in which the 1/5DNP38C10 macrocycle resides on the NpI unit. In order to induce the rotaxane to switch, an excess of $LiClO_4$ dissolved in ~200 μL of CD_3COCD_3 was added to the sample, which was then shaken vigorously to ensure complete mixing of the two solutions in the NMR sample tube. After addition of the $LiClO_4$, the ^1H NMR spectrum was recorded (Figure 21b) again at room temperature. Comparing this spectrum (Figure 21b) with that (Figure 21a) for the rotaxane, prior to addition of the lithium salt, reveals some distinct changes in chemical shifts. The signal at $\delta = 8.19$ ppm for the protons (H_{Np}) of the encircled NpI unit is absent and signals for the "uncomplexed" NpI unit (H_{Np}) appear at $\delta = 8.62$ and 8.66 ppm. Also, the signal corresponding to the "uncomplexed" PmI unit (H_{Pm}) at $\delta = 8.24$ ppm is no longer present in the spectrum. Unfortunately, the signal corresponding to the encircled PmI unit (H_{Pm}) is obscured by the other aromatic signals.

Further support for the presence of essentially only a single translational isomer before and after addition of $LiClO_4$ can be obtained by examining the signals corresponding to the methyl groups of the hydrophobic stopper (see the expansion in Figure 21). Both of the major translational isomers possess two constitutionally distinct stoppers as a result of the two different recognition sites within the dumbbell. A consequence is that all of the signals for the protons of the stoppers should appear in the form of two equal-intensity signals, assuming the ring is located solely on one of the two recognition sites. These signals can be seen clearly in the expansions, in which the methyl groups of the *tert*-butyl group give rise to two singlets, while the methyl groups of the isopropyl group give rise to two doublets, both before and after addition of the lithium salt.

Another more subtle indication of the nature of the lithium complex comes from the change of the NpI signals.

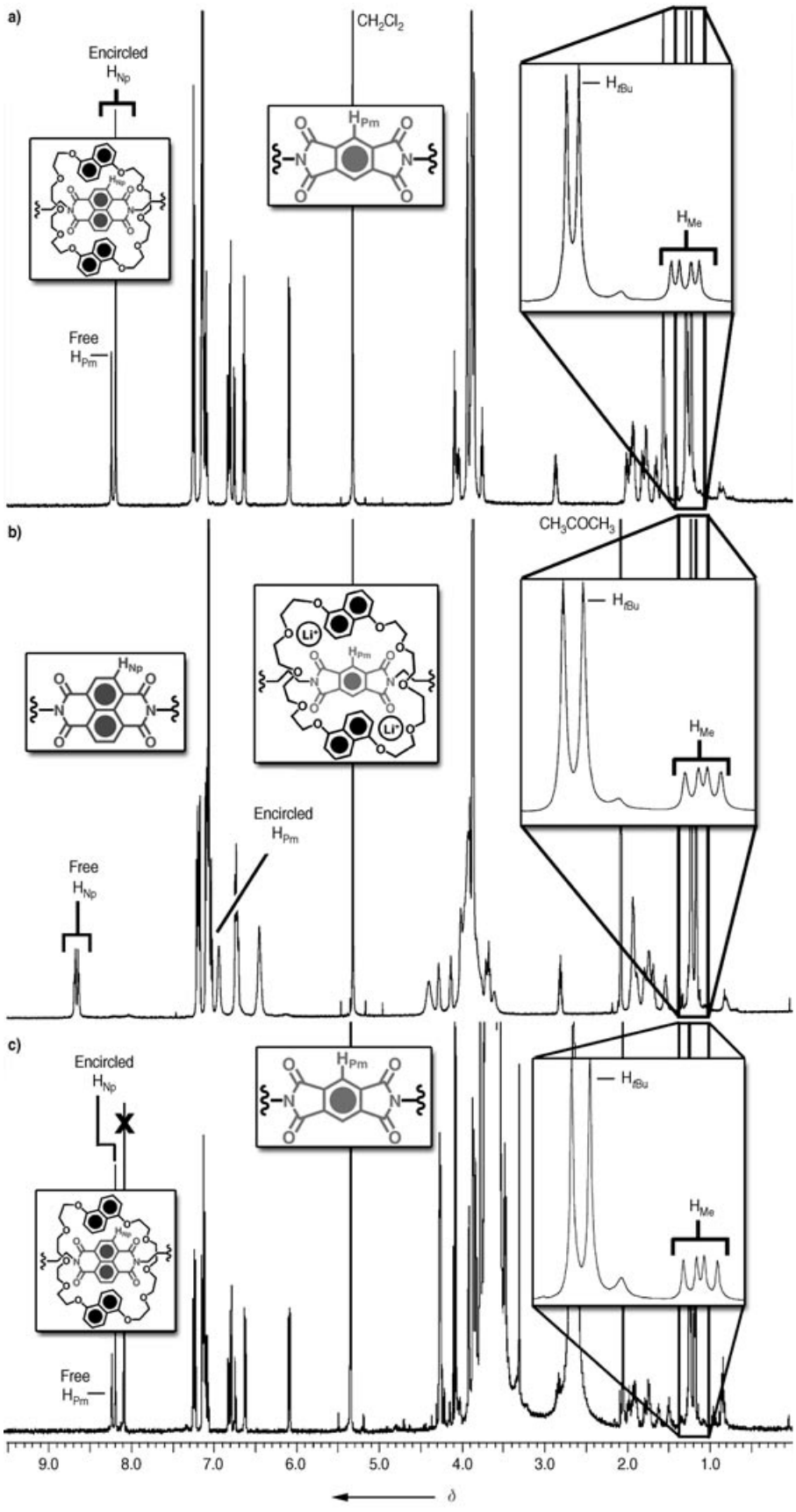

Figure 21. ^{1}H NMR spectra (600 MHz) of **NpPmR** at room temperature in CD_2Cl_2 a) before and b) after addition of excess of $LiClO_4$ dissolved in 200 μL of CD_3COCD_3. The insets show the partial structures for the rotaxane before and after addition of the lithium. The expansion shows the signals corresponding to the methyl groups on the hydrophobic stopper.

Before addition of lithium salt, the NpI unit gives rise to one peak at $\delta = 8.19$ ppm. After addition of $LiClO_4$, however, two doublets are observed at $\delta =$ 8.62 and 8.66 ppm. This difference in chemical shift arises from the fact that the two ends of the NpI unit are not constitutionally the same—see Figure 10, in which the squares and triangles represent different structural entities attached to the NpI unit. Although this separation exists both before and after addition of the lithium salt, the presence of the Li^+ ions accentuates the constitutional heterotopicity of the two ends, causing the $\Delta\delta$ value to be larger and thus making it easier to observe. Before addition of the lithium salt, the $\Delta\delta$ value is so small that they appear as only a single resonance.

To determine if this ion-induced switching process was reversible, [12]crown-4 is added to the sample after recording the spectrum of the switched rotaxane. This crown ether acts as a sequestering agent[38] for Li^+ ions and competes with the rotaxane for binding to the Li^+ ions. An excess of [12]crown-4 was added to drive the equilibrium completely towards the Li^+·[12]crown-4 complex, returning the rotaxane to its neutral ground state. The ^{1}H NMR spectrum (Figure 21c) of the solution containing the rotaxane, $LiClO_4$, and excess [12]crown-4 was then recorded . The signal at $\delta = 8.1$ ppm arises from an impurity present in the commercial sample of [12]crown-4. Other than a slight upfield shift for some of the signals, presumably caused by a change in the polarity of the solvent, the observable signals are the same as those for the neutral ground-state rotaxane, indicating that the switching process has been reversed.

Conclusion

Important and successful steps have been taken towards the design, synthesis, and characterization of redox-controlled donor–acceptor, neutral [2]rotaxanes that could fulfill the role of switches in a future generation of molecular electronic devices. NMR spectroscopic and photophysical investigations have demonstrated quite independently and beyond any shadow of a doubt, that, in the nondegenerate [2]rotaxane **NpPmR** with both PmI and NpI recognition sites located along the rod section of the dumbbell component, by far the most stable translational isomer is the one in which the 1/5DNP38C10 macrocycle encircles the NpI recognition site, which is itself a much better electron acceptor than the PmI one. Furthermore, a detailed electrochemical investigation of the redox-controllable, donor–acceptor, bistable [2]rotaxane reveals that, upon one-electron reduction, its NpI recognition site is deactivated and the 1/5DNP38C10 macrocycle moves to the PmI one. Also, it is worthy of note that when this second recognition site is deactivated by electrochemical reduction, the 1/5DNP38C10 macrocycle apparently is no longer involved in any donor–acceptor interactions. This electrochemical behavior is just what is wanted in a nanoelectromechanical switch, that is, there exists the potential to destabilize the metastable state of a bistable switch (Figure 3). All that is needed now is to introduce amphiphilicity[7] into this neutral bistable [2]rotaxane so that it can be self-organized as a Langmuir film[8,9] and transferred as a molecular monolayer by means of the Langmuir–Blodgett technique into a two-terminal crossbar device.[6] This research goal is being pursued presently with some vigor as we seek to broaden the scope of bistable rotaxanes in molecular electronic devices from charged tetracationic systems[6–11] to neutral molecules.

Research rarely happens without throwing up a few surprises and presenting the odd bonus to the researchers. This collaborative venture has been no exception in so far as it has uncovered a practical way by which the neutral bistable [2]rotaxane can also be switched chemically using lithium cations. The ability of two Li^+ ions to form a 2:1 co-complex in solution with pseudorotaxanes,[36] self-assembled between substrates that contain electron-accepting diimide (PmI or NpI) units and the electron-donating 1/5DNP38C10 macrocycle acting as a receptor, can be used to switch **NpPmR**. Since the pole-dipole interactions involving the Li^+ ions and the oxygen atoms in the polyether loops of the 1/5DNP38C10 macrocycle are stronger in the case of a PmI-encircled unit, addition of Li^+ ions to the neutral bistable [2]rotaxane induces the 1/5DNP38C10 macrocycle to move from the NpI to the PmI recognition site. This observation is a significant one in the context of the future design and operation of artificial (supra)molecular machines[4,39] that will be driven by some kind of chemomechanical mechanism.[40]

Experimental Section

General methods: Chemicals were purchased from Aldrich or TCI and used as received. The compounds 4-[4-isopropylphenylbis(4-*tert*-butylphenyl)methyl]phenol[20] (**1**) , 5-[(tetrahydropyan-2-yl)oxy]pentan-1-ol[22] (**4**), 1,5-dinaphtho[38]crown-10,[23] (**6**) and 1,4,5,8-naphthalenecarboxylic diimide[24] (**7**) were all prepared according to literature procedures. Solvents were dried following methods described in the literature.[25] All reactions were carried out under an anhydrous argon atmosphere. Thin-layer chromatography (TLC) was performed on aluminum sheets, coated with silica-gel 60F (Merck 5554). The plates were inspected by UV light and, if required, developed in I_2 vapor. Column chromatography was carried out by using silica-gel 60 (Merck 9385, 230–400 mesh). Melting points were determined on an Electrothermal 9100 melting point apparatus and are uncorrected. All ^1H and ^{13}C NMR spectra were recorded on either 1) a Bruker ARX400 (400 MHz and 100 MHz, respectively), 2) a Bruker ARX500 (500 MHz and 125 MHz, respectively), or 3) a Bruker Avance500 (500 MHz and 125 MHz, respectively), with residual solvent as the internal standard. Samples were prepared in $CDCl_3$ and CD_3OD purchased from Cambridge Isotope Labs. All chemical shifts are quoted using the δ scale, and all coupling constants (J) are expressed in Hertz (Hz). Fast atom bombardment (FAB) mass spectra were obtained using a ZAB-SE mass spectrometer, equipped with a krypton primary atom beam utilizing a *m*-nitrobenzyl alcohol matrix. Cesium iodide or poly(ethylene glycol) were employed as reference compounds. Matrix-assisted laser-desorption ionization time-of-flight (MALDI-TOF) mass spectra were measured on an IonSpec Fourier transform mass spectrometer.

Photophysical experiments: All measurements were performed at room temperature in air-equilibrated CH_2Cl_2 (Merck Uvasol™) solutions (2×10^{-5}–1×10^{-4} M). UV-visible absorption spectra were recorded with a Perkin–Elmer Lambda 40 spectrophotometer. Uncorrected fluorescence spectra were obtained with a Perkin–Elmer LS-50 spectrofluorimeter, equipped with a Hamamatsu R928 phototube. Naphthalene in air-equilibrated cyclohexane ($\Phi=0.036$)[41] was used as the standard for evaluating the luminescence quantum yields. The estimated experimental errors are: 2 nm on band maxima, ±10% on the molar absorption coefficients and fluorescence intensity.

Electrochemical experiments: Cyclic voltammetric (CV) and differential pulse voltammetric (DPV) experiments were carried out in argon-purged CH_2Cl_2 (Romil Hi-Dry™) at room temperature with an Autolab 30 multipurpose instrument interfaced to a personal computer. The working electrode was a glassy carbon electrode (0.08 cm^2, Amel); its surface was routinely polished with 0.3 μm alumina–water slurry on a felt surface, immediately prior to use. In all cases, the counterelectrode was a Pt spiral, separated from the bulk solution with a fine glass frit, and an Ag wire was used as a quasi-reference electrode. Ferrocene ($E_{1/2}=-0.46$ V vs SCE in CH_2Cl_2)[42] was present as the internal standard. In all the electrochemical experiments the concentration of the compounds was in the range 5×10^{-4}–1×10^{-3} M and tetrabutylammonium hexafluorophosphate solution of a 100 times higher concentration was added as supporting electrolyte. Cyclic voltammograms were obtained with sweep rates in the range 0.02–1.0 Vs^{-1}; the IR compensation implemented within the Autolab 30 was used, and every effort was made throughout the experiments in order to minimize the resistance of the solution. In any instance, the full reversibility of the voltammetric wave of ferrocene was taken as an indicator of the absence of uncompensated resistance effects. The DPV experiments were performed with a scan rate of 20 or 4 $mV\,s^{-1}$ (pulse height 75 and 10 mV, respectively) and a duration of 40 ms. The reversibility of the observed processes was established by using the criteria of 1) separation of 60 mV between cathodic and anodic peaks, 2) the close to unity ratio of the intensities of the cathodic and anodic currents, and 3) the constancy of the peak potential on changing sweep rate in the cyclic voltammograms. The same halfwave potential values were obtained from the DPV peaks and from an average of the cathodic and anodic CV peaks, as expected for reversible processes. The number of exchanged electrons in the redox processes of the investigated dumbbells and [2]rotaxanes was measured by comparing the current intensity of the CV waves and the area of the DPV peaks with those found for the two reversible and monoelectronic reduction processes of the model compounds **9** and **10**, after correction for differences in the diffusion coefficients and concentrations.[43] The experimental errors associated with the potential values were estimated to be ±10 mV. Digital simulation of the experimental CVs were obtained by using the software package DigiSim 3.05.[44]

Compound 2: A solution of 5-chloro-1-pentanol (999 mg, 8.15 mmol), **1** (2.00 g, 4.08 mmol), K_2CO_3 (1.69 g, 12.23 mmol), LiBr (10 mg, cat. amount), and [18]crown-6 (10 mg, cat. amount) in dry MeCN (80 mL) was heated under reflux for 6 d. After cooling down to room temperature, the reaction mixture was filtered and the residue was washed with MeCN (50 mL). The combined organic phase was concentrated in vacuo and the crude product was purified by column chromatography (SiO_2: CH_2Cl_2) to give **2** (1.95 g, 83%) as a white solid. M.p. 190–192°C; ^{1}H NMR ($CDCl_3$, 400 MHz): δ=1.23 (d, J=6.9 Hz, 6H), 1.31 (s, 18H), 1.52–1.68 (m, 4H), 1.79–1.83 (m, 2H), 2.89 (septet, J=6.9 Hz, 1H), 3.66 (t, J=6.5 Hz, 2H), 3.95 (t, J=6.4 Hz, 2H), 6.76 (d, J=8.9 Hz, 2H), 7.08–7.15 (m, 10H), 7.23 ppm (d, J=8.6 Hz, 4H); ^{13}C NMR ($CDCl_3$, 400 MHz): δ=22.4, 24.0, 29.1, 31.4, 32.5, 33.5, 34.3, 62.8, 63.2, 67.6, 113.0, 124.1, 125.2, 130.8, 131.0, 132.2, 139.5, 144.2, 144.7, 146.0, 148.3, 156.8 ppm; MS (FAB): m/z (%): 576 (55)$[M]^+$, 457(45), 443(80), 397 (100); elemental analysis calcd (%) for $C_{41}H_{52}O_2$ (576): C 85.37, H 9.09; found: C 85.08, H 9.33.

Compound 5: DEAD (700 mg, 4.02 mmol) was added dropwise at 0°C under an Ar atmosphere to a solution of **2** (1.16 g, 2.01 mmol), **3** (478 mg, 2.21 mmol), **4** (379 mg, 2.01 mmol), and PPh_3 (1.06 g, 4.02 mmol) in THF (50 mL); the reaction mixture was stirred at room temperature for 16 h. The mixture was filtered though silica gel and the solution was evaporated in vacuo to obtain a crude product, which was then purified by column chromatography (SiO_2: CH_2Cl_2/Me_2CO, 100:3). The colorless band (R_f=0.5) was collected and dissolved in MeOH/CH_2Cl_2 (1:1, 100 mL). A concentrated HCl aqueous solution (0.5 mL) was added and the reaction mixture was stirred at room temperature for 4 h. After removal of the solvent, the residue was purified by column chromatography (SiO_2: CH_2Cl_2/Me_2CO, 100:5) to give **5** (0.65 g, 37%) as a yellow solid. M.p. 239–241°C; ^{1}H NMR ($CDCl_3$, 400 MHz): δ=1.23 (d, J=6.9 Hz, 6H), 1.29 (s, 18H), 1.41–1.54 (m, 4H), 1.60–1.67 (m, 2H), 1.72–1.85(m, 6H), 2.86 (septet, J=6.9 Hz, 1H), 3.65 (t, J=6.5 Hz, 2H), 3.73–3.80 (m, 4H), 3.92(t, J=6.2 Hz, 2H), 6.73 (d, J=8.6 Hz, 2H), 7.05–7.10 (m, 10H), 7.23 (d, J=8.6 Hz, 4H), 8.27 ppm (s, 2H); ^{13}C NMR ($CDCl_3$, 400 MHz): δ=23.1, 23.6, 24.0, 28.2, 28.9, 31.4, 32.1, 33.5, 34.3, 38.6 41.7, 62.6, 63.1, 67.3, 112.9, 118.2, 124.1, 125.2, 129.1, 130.7, 131.0, 132.2, 137.2, 139.6, 144.2, 144.6, 146.0, 148.3, 156.7, 166.3, 166.3 ppm; MS (MALDI-TOF): m/z calcd for $C_{56}H_{64}N_2O_6Na$: 883.5; found: 883.6; elemental analysis calcd (%) for $C_{56}H_{64}N_2O_6$ (860): C 78.11; H 7.49, N 3.25; found: C 77.89, H 7.59, N 3.24.

Dumbbell PmPmD: DEAD (181 mg, 1.04 mmol) was added dropwise at 0°C under an Ar atmosphere to a solution of **2** (300 mg, 0.52 mmol), **3** (124 mg, 0.57 mmol), **5** (448 mg, 0.52 mmol), and PPh_3 (273 mg, 1.04 mmol) in THF (20 mL) and the reaction mixture was stirred at room temperature for 2 d. The mixture was filtered though silica gel and the solution was evaporated in vacuo to obtain a crude product, which was then purified by column chromatography (SiO_2: CH_2Cl_2/Me_2CO, 100:5) to give **PmPmD** (0.28 g, 33%) as a yellow solid. M.p. 213–216°C; ^{1}H NMR ($CDCl_3$, 400 MHz): δ=1.24 (d, J=6.9 Hz, 12H), 1.30 (s, 36H), 1.50–1.60 (m, 6H), 1.73–1.90(m, 12H), 2.87 (septet, J=6.9 Hz, 2H), 3.70–3.82 (m, 8H), 3.93 (t, J=6.3 Hz, 4H), 6.73 (d, J=8.9 Hz, 4H), 7.05–7.10 (m, 20H), 7.23 (d, J=8.6 Hz, 8H), 8.21 ppm (s, 4H); ^{13}C NMR ($CDCl_3$, 400 MHz): δ=23.6, 24.0, 27.8, 28.3, 28.9, 31.4, 34.3, 38.2, 38.6, 63.1, 67.3, 112.9, 118.2, 124.1, 125.2, 130.7, 131.0, 132.2, 137.2, 137.3, 139.6, 144.2, 144.6, 146.0, 148.3, 156.7, 166.2, 166.3 ppm; MS (MALDI-TOF): m/z calcd for $C_{107}H_{116}N_4O_{10}$: 1617; found: 1640 $[M+Na]^+$; HRMS (MALDI-TOF): m/z calcd for $C_{107}H_{116}N_4O_{10}Na$: 1640.8622; found: 1640.8666 .

Rotaxane PmPmR: A solution of **PmPmD** (48.5 mg, 0.03 mmol), **6** (95.5 mg, 0.15 mmol), and LiBr (13.0 mg, 0.15 mmol) in $CHCl_3$/MeOH (95:5, 1 mL) was heated at 60°C for 14 d. After cooling down to room temperature, the mixture was evaporated in vacuo to obtain a crude product which was then purified by column chromatography (SiO_2: $CHCl_3$/EtOAc, 80:20) to give **PmPmR** (29.6 mg, 44%) as a yellow solid. M.p. 196–197°C; ^{1}H NMR ($CDCl_3$, 500 MHz): δ=1.23 (d, J=6.9 Hz, 12H), 1.29 (s, 36H), 1.53–1.65 (m, 6H), 1.78–1.94 (m, 12H), 2.87 (septet, J=6.9 Hz, 2H), 3.63–3.73 (m, 8H), 3.90–4.10 (m, 36H), 6.28 (d, J=7.6 Hz, 4H), 6.70–6.79 (m, 8H), 7.05–7.10 (m, 20H), 7.17 (d, J=8.4 Hz, 4H), 7.21 (d, J=8.6 Hz, 8H), 7.55–7.75 ppm (br, 4H); ^{13}C NMR ($CDCl_3$, 500 MHz): δ=23.7, 23.8, 24.3, 28.1, 28.3, 28.8, 29.6, 31.2, 33.3, 34.2, 38.0, 38.2, 63.0, 67.3, 67.8, 69.4, 71.1, 71.2, 104.4, 112.8, 113.9, 116.9, 123.9, 124.0, 125.0, 125.3, 130.6, 130.9, 132.1, 135.3, 139.5, 144.0, 144.5, 145.8, 148.1, 153.5, 156.6, 166.1, 166.2 ppm; MS (FAB): m/z (%): 576 (55) $[M]^+$, 457(45), 443(80), 397 (100); MS (MALDI-TOF): m/z calcd for $C_{143}H_{160}N_4O_{20}$: 2254; found: 2277 $[M+Na]^+$; HRMS (MALDI-TOF): m/z calcd for $C_{143}H_{160}N_4O_{20}Na$: 2277.1557; found: 2277.1570.

Compound 8: DEAD (724 mg, 4.16 mmol) was added dropwise at 0°C under an Ar atmosphere to a solution of **2** (1.20 g, 2.08 mmol), **4** (392 mg, 2.08 mmol), **7** (609 mg, 2.29 mmol), and PPh_3 (1.09 g, 4.16 mmol) in THF (50 mL); the reaction mixture was stirred at room temperature for 16 h. The mixture was filtered though silica gel and the solution was evaporated in vacuo to obtain a crude product, which was then purified by column chromatography (SiO_2: CH_2Cl_2/Me_2CO, 100:3). The colorless band (R_f=0.6) was collected and dissolved in MeOH/CH_2Cl_2 (1:1, 100 mL). A concentrated HCl aqueous solution (0.5 mL) was added and the reaction mixture was stirred at room temperature for 4 h. After removal of the solvent, the residue was purified by column chromatography (SiO_2: CH_2Cl_2/Me_2CO, 100:5) to give **8** (0.63 g, 33%) as a yellow solid. M.p. 257–259°C; ^{1}H NMR ($CDCl_3$, 500 MHz): δ=1.23 (d, J=6.9 Hz, 6H), 1.30 (s, 18H), 1.50–1.70 (m, 6H), 1.76–1.88 (m, 6H), 2.86 (septet, J=6.9 Hz, 1H), 3.68 (t, J=6.4 Hz, 2H), 3.95 (t, J=6.3 Hz, 2H), 4.22 (q, J=7.1 Hz, 4H), 6.73 (d, J=8.9 Hz, 2H), 7.05–7.10 (m, 10H), 7.22 (d, J=8.6 Hz, 4H), 8.75 ppm (s, 4H); ^{13}C NMR ($CDCl_3$, 400 MHz): δ= 23.3, 23.7, 23.4, 27.8, 27.9, 29.1, 31.4, 32.3, 33.5, 34.3, 40.8, 62.7, 63.1, 67.4, 113.0, 124.0, 125.2, 126.6, 126.62, 126.7 130.7, 131.0, 132.2, 139.5, 144.2, 144.6, 146.0, 148.3, 156.8, 162.8, 162.9 ppm; MS (MALDI-TOF): m/z calcd for $C_{60}H_{66}N_2O_6Na$: 933.5; found: 933.7; HRMS (MALDI-TOF): m/z calcd for $C_{60}H_{66}N_2O_6Na$: 933.4813; found: 933.4803.

Dumbbell NpNpD: DEAD (169 mg, 0.97 mmol) was added dropwise at 0°C under an Ar atmosphere to a solution of **2** (280 mg, 0.49 mmol), **7** (142 mg, 0.53 mmol), **8** (442 mg, 0.49 mmol), and PPh_3 (255 mg, 0.97 mmol) in THF (20 mL); the reaction mixture was stirred at room temperature for 2 d. The mixture was filtered though silica gel and the solution was evaporated in vacuo to obtain the crude product which was then purified by column chromatography (SiO_2: CH_2Cl_2/Me_2CO, 100:5) to give **NpNpD** (0.35 g, 40%) as a orange solid. M.p. 190–192°C; ^{1}H NMR ($CDCl_3$, 400 MHz): δ=1.23 (d, J=6.9 Hz, 12H), 1.30 (s, 36H), 1.53–1.70 (m, 6H), 1.76–1.90 (m, 12H), 2.86 (septet, J=6.9 Hz, 2H), 3.96 (t, J=6.3 Hz, 4H), 4.22 (m, 8H), 6.74 (d, J=8.9 Hz, 4H), 7.05–7.10 (m, 20H), 7.23 (d, J=8.6 Hz, 8H), 8.73 ppm (AA'BB' system, 8H); ^{13}C NMR ($CDCl_3$, 400 MHz): δ=23.7, 24.0, 27.7, 27.9, 31.4, 33.4, 34.3, 40.7, 63.1, 67.4, 112.9, 124.0, 125.2, 126.6, 126.7, 130.9, 131.0, 132.2, 139.5, 144.2, 144.6, 146.0, 148.3, 156.8, 162.8 ppm; MS (MALDI-TOF): m/z calcd for $C_{115}H_{120}N_4O_{10}$: 1717; found: 1718 $[M+H]^+$; HRMS (MALDI-TOF): m/z calcd for $C_{115}H_{121}N_4O_{10}$: 1717.9083; found: 1717.9077 $[M+H]^+$.

Rotaxane NpNpR: A solution of **NpNpD** (51.5 mg, 0.03 mmol), **6** (95.5 mg, 0.15 mmol), and LiBr (13.0 mg, 0.15 mmol) in $CHCl_3$/MeOH (95:5, 1 mL) was heated at 60°C for 14 d. After cooling down to room temperature, the mixture was evaporated in vacuo to obtain a crude product which was then purified by column chromatography (SiO_2: $CHCl_3$/EtOAc, 80:20) to give **NpNpR** (30 mg, 42%) as a violet solid. M.p. 212–214°C; ^{1}H NMR ($CDCl_3$, 500 MHz): δ=1.23 (d, J=6.9 Hz, 12H), 1.29 (s, 36H), 1.59–1.79 (br, 6H), 1.81–2.07 (br, 12H), 2.87 (septet, J=6.9 Hz, 2H), 3.77–4.33 (m, 44H), 6.07 (d, J=7.6 Hz, 4H), 6.60–6.65 (m, 4H), 6.76–6.81 (br, 4H), 6.83 (d, J=8.4 Hz, 4H), 7.05–7.10 (m, 20H), 7.22 (d, J=8.6 Hz, 8H), 8.00–9.00 ppm (br, 8H); ^{13}C NMR ($CDCl_3$, 500 MHz): δ=23.9, 24.8, 27.7, 27.8, 31.3, 33.3, 34.2, 40.4, 63.0, 67.2, 67.4, 69.7, 71.0, 71.2, 103.2, 112.8, 113.9, 123.4, 123.9, 124.6, 125.0, 130.6, 130.9, 132.1, 139.4, 144.1, 144.5, 145.8, 148.1, 152.9, 156.7, 162.8 ppm; MS (FAB): m/z (%): 576 (55) $[M]^+$, 457(45), 443(80), 397 (100); MS (MALDI-TOF): m/z calcd for $C_{151}H_{164}N_4O_{20}$: 2354; found: 2377 $[M+Na]^+$; HRMS (MALDI-TOF): m/z calcd for $C_{151}H_{164}N_4O_{20}Na$: 2377.1870; found: 2377.2567.

Dumbbell NpPmD: DEAD (121 mg, 0.69 mmol) was added dropwise at 0°C under an Ar atmosphere to a solution of **2** (200 mg, 0.35 mmol), **5** (299 mg, 0.35 mmol), **7** (102 mg, 0.38 mmol), and PPh_3 (182 mg, 0.69 mmol) in THF (20 mL); the reaction mixture was stirred at room temperature for 2 d. The mixture was filtered though silica gel and the solution was evaporated in vacuo to obtain the crude product which was then purified by column chromatography (SiO_2: CH_2Cl_2/EtOAc, 90:10) to give **NpPmD** (0.17 g, 30%) as a yellow solid. M.p. 168–170°C; ^{1}H NMR ($CDCl_3$, 500 MHz): δ=1.23 (d, J=6.9 Hz, 12H), 1.30 (s, 36H),

1.46–1.67 (m, 6H), 1.75–1.91 (m, 12H), 2.86 (septet, $J=7.0$ Hz, 2H), 3.74–3.82 (m, 4H), 3.90–3.98 (m, 4H), 4.18–4.28 (m, 4H), 6.71–6.77 (m, 4H), 7.05–7.12 (m, 20H), 7.23 (d, $J=8.4$ Hz, 8H), 8.13 (s, 2H), 8.74 ppm (AA′BB′ system, 4H); ^{13}C NMR ($CDCl_3$, 500 MHz): $\delta=23.5$, 23.6, 23.9, 24.1, 27.3, 27.8, 27.9, 28.1, 28.8, 29.0, 31.3, 31.5, 33.3, 34.2, 38.2, 38.5, 40.4, 40.7, 63.0, 67.2, 67.3, 112.8, 112.9, 118.0, 123.9, 125.1, 126.4, 126.6, 130.6, 130.9, 132.1, 137.1, 139.4, 139.4, 144.0, 144.1, 144.5, 145.9, 148.1, 156.6, 156.7, 162.6, 162.7, 166.1 ppm; MS (MALDI-TOF): *m*/*z* calcd for $C_{111}H_{118}N_4O_{10}$: 1667; found: 1690 $[M+Na]^+$; HRMS (MALDI-TOF): *m*/*z* calcd for $C_{111}H_{118}N_4O_{10}Na$: 1689.8746; found: 1689.8730.

Rotaxane NpPmR: A solution of **NpPmD** (25.0 mg, 0.015 mmol), **6** (47.8 mg, 0.075 mmol), and LiBr (6.5 mg, 0.075 mmol) in $CHCl_3$/MeOH (95:5, 1 mL) was heated at 60 °C for 14 d. After cooling down to room temperature, the mixture was evaporated in vacuo to obtain a crude product which was then purified by column chromatography (SiO_2: $CHCl_3$/EtOAc, 80:20) to give **NpPmR** (18 mg, 52 %) as a orange solid. M.p. 193–196 °C; ^{1}H NMR ($CDCl_3$, 500 MHz): $\delta=1.23$ (dd, $J=6.9$, 1.5 Hz, 12H), 1.29 (d, $J=2.5$ Hz, 36H), 1.52–1.67 (m, 4H), 1.72–1.88 (m, 6H), 1.88–2.04 (m, 8H), 2.87 (m, 2H), 3.77 (t, $J=7.3$ Hz, 2H), 3.83–4.12 (m, 42H), 6.07 (d, $J=7.6$ Hz, 4H), 6.62 (t, $J=8.0$ Hz, 4H), 6.72 (d, $J=8.4$ Hz, 2H), 6.82 (d, $J=8.4$ Hz, 4H), 7.05–7.10 (m, 20H), 7.18–7.27 (m, 8H), 8.20–8.30 ppm (br, 6H); ^{13}C NMR ($CDCl_3$, 500 MHz): $\delta=23.5$, 23.8, 24.1, 24.5, 27.4, 27.8, 28.2, 28.8, 29.1, 31.3, 33.3, 34.2, 38.4, 38.5, 40.0, 40.2, 63.0, 67.2, 67.3, 67.5, 69.7, 71.1, 71.2, 103.3, 112.8, 112.9 113.9, 118.0,123.4, 123.9, 124.6, 124.9, 125.0, 125.1, 130.3, 130.4, 130.6, 130.9, 132.1, 132.2, 137.1, 139.4, 139.5, 144.1, 144.5, 145.8, 145.9, 148.1, 148.2, 152.9, 156.6, 156.7, 162.9, 163.0, 166.1, 166.2 ppm; MS (MALDI-TOF): *m*/*z* calcd for $C_{147}H_{162}N_4O_{20}$: 2303; found: 2304 $[M+H]^+$; HRMS (MALDI-TOF): *m*/*z* calcd for $C_{151}H_{165}N_4O_{20}$: 2304.1860; found: 2304.1855.

Acknowledgements

This research was supported at the University of California, Los Angeles by the Defense Advanced Research Project Agency (DARPA) and in part by the National Science Foundation under equipment grant CHE-9974928. T.I. thanks the JSR Corporation for a visiting scholar fellowship. This research was supported at the University of Bologna by the FIRB (Manipolazione molecolare per macchine nanometriche) and the European Union through the Molecular-Level Devices and Machines Network (HPRN-CT-2000–00029). The research was supported at the University of Cambridge by the Engineering and Physical Sciences Research Council.

[1] a) J.-M. Lehn, *Supramolecular Chemistry*, VCH, Weinheim, **1995**; b) M. C. T. Fyfe, J. F. Stoddart, *Acc. Chem. Res.* **1997**, *30*, 393–401; c) H.-J. Schneider, A. Yatsimirsky, *Principles and Methods in Supramolecular Chemistry*, Wiley-VCH, Weinheim, **2000**; d) J. W. Steed, J. L. Atwood, *Supramolecular Chemistry*, Wiley-VCH, Weinheim, **2000**; e) J.-M. Lehn, *Science*, **2002**, *295*, 2400–2403; f) D. N. Reinhoudt, M. Crego-Calama, *Science* **2002**, *295*, 2403–2407; g) P. A. Gale, *Annu. Rep. Prog. Chem. Sect. B* **2003**, *99*, 244–262.

[2] a) S. Anderson, H. L. Anderson, J. K. M. Sanders, *Acc. Chem. Res.* **1993**, *26*, 469–475; b) R. Jäger, F. Vögtle, *Angew. Chem.* **1997**, *109*, 966–980; *Angew. Chem. Int. Ed. Engl.* **1997**, *36*, 930–944; c) G. A. Breault, C. A. Hunter, P. C. Mayers, *Tetrahedron* **1999**, *55*, 5265–5293; d) *Templated Organic Synthesis* (Eds.: F. Diederich, P. J. Stang), Wiley-VCH, Weinheim, **1999**; e) "Self-Assembly in Supramolecular Systems": L. F. Lindoy, I. M. Atkinson, in *Monographs in Supramolecular Chemistry* (Ed.: J. F. Stoddart), Royal Society of Chemistry, Cambridge, **2000**; f) J. F. Stoddart, H.-R. Tseng, *Proc. Natl. Acad. Sci. USA* **2002**, *99*, 4797–4800; g) L. Raehm, D. G. Hamilton, J. K. M. Sanders, *Synlett* **2002**, 1743–1761.

[3] a) J. F. Stoddart, *Chem. Aust.* **1992**, *59*, 576–577 and 581; b) M. Gómez-López, J. A. Preece, J. F. Stoddart, *Nanotechnology* **1996**, *7*, 183–192; c) V. Balzani, M. Gómez-López, J. F. Stoddart, *Acc. Chem. Res.* **1998**, *31*, 405–414; d) V. Balzani, A. Credi, F. M. Raymo, J. F. Stoddart, *Angew. Chem.* **2000**, *112*, 3484–3530; *Angew. Chem. Int. Ed.* **2000**, *39*, 3348–3391; e) H.-R. Tseng, J. F. Stoddart, in *Modern Arene Chemistry* (Ed.: D. Astruc), Wiley-VCH, **2002**, 574–599.

[4] a) A. Harada, *Acc. Chem. Res.* **2001**, *34*, 456–464; b) C. A. Schalley, K. Beizai, F. Vögtle, *Acc. Chem. Res.* **2001**, *34*, 465–476; c) J.-P. Collin, C. Dietrich-Buchecker, P. Gaviña, M. C. Jimenez-Molero, J.-P. Sauvage, *Acc. Chem. Res.* **2001**, *34*, 477–487; d) R. Ballardini, V. Balzani, A. Credi, M. T. Gandolfi, M. Venturi, *Struct. Bonding* **2001**, *99*, 55–78; e) C. A. Stainer, S. J. Alderman, T. D. W. Claridge, H. L. Anderson, *Angew. Chem.* **2002**, *114*, 1847–1850; *Angew. Chem. Int. Ed.* **2002**, *41*, 1769–1772; f) V. Balzani, A. Credi, M. Venturi, *Chem. Eur. J.* **2002**, *8*, 5524–5532; g) V. Balzani, A. Credi, M. Venturi, *Molecular Devices and Machines—A Journey into the Nano World*, Wiley-VCH, Weinheim, **2003**; h) C. Dietrich-Buchecker, M. C. Jimenez-Molero, V. Sartor, J.-P. Sauvage, *Pure Appl. Chem.* **2003**, *75*, 1383–1393.

[5] a) T. J. Huang, A. H. Flood, C.-W. Chu, S. Kang, T.-F. Guo, T. Yamamoto, H.-R. Tseng, B.-D. Yu, Y. Yang, J. F. Stoddart, C.-M. Ho, *IEEE* **2003**, *2*, 698–701; b) T. J. Huang, H.-R. Tseng, L. Sha, W. Lu, B. Brough, A. H. Flood, B.-D. Yu, P. C. Celestre, J. P. Chang, J. F. Stoddart, C.-M. Ho, *NanoLett* **2004**, *4*, in press.

[6] a) C. P. Collier, G. Mattersteig, E. W. Wong, Y. Luo, K. Beverly, J. Sampaio, F. M. Raymo, J. F. Stoddart, J. R. Heath, *Science* **2000**, *289*, 1172–1175; b) A. R. Pease, J. O. Jeppesen, J. F. Stoddart, Y. Luo, C. P. Collier, J. R. Heath, *Acc. Chem. Res.* **2001**, *34*, 433–444; c) Y. Luo, C. P. Collier, J. O. Jeppesen, K. A. Nielsen, E. DeIonno, G. Ho, J. Perkins, H.-R. Tseng, T. Yamamoto, J. F. Stoddart, J. R. Heath, *ChemPhysChem* **2002**, *3*, 519–525; d) M. R. Diehl, D. W. Steuerman, H.-R. Tseng, S. A. Vignon, A. Star, P. C. Celestre, J. F. Stoddart J. R. Heath, *ChemPhysChem* **2003**, *4*, 1335–1339; e) H. Yu, Y. Luo, K. Beverly, H.-R. Tseng, J. F. Stoddart, J. R. Heath, *Angew. Chem.* **2003**, *115*, 5884–5889; *Angew. Chem. Int. Ed.* **2003**, *42*, 5706–5711.

[7] a) J. O. Jeppesen, K. A. Nielsen, J. Perkins, S. A. Vignon, A. Di Fabio, R. Ballardini, M. T. Gandolfi, M. Venturi, V. Balzani, J. Becher, J. F. Stoddart, *Chem. Eur. J.* **2003**, *9*, 2982–3007; b) T. Yamamoto, H.-R. Tseng, J. F. Stoddart, V. Balzani, A. Credi, F. Marchioni, M. Venturi, *Collect. Czech. Chem. Commun.* **2003**, *68*, 1488–1514; c) H.-R. Tseng, S. A. Vignon, P. C. Celestre, J. Perkins, J. O. Jeppesen, A. Di Fabio, R. Ballardini, M. T. Gandolfi, M. Venturi, V. Balzani, J. F. Stoddart, *Chem. Eur. J.* **2004**, *10*, 155–172.

[8] C. P. Collier, J. O. Jeppesen, Y. Luo, J. Perkins, E. W. Wong, J. R. Heath, J. F. Stoddart, *J. Am. Chem. Soc.* **2001**, *123*, 12632–12641.

[9] a) I. C. Lee, C. W. Frank, T. Yamamoto, H.-R. Tseng, A. H. Flood, J. F. Stoddart, *Langmuir*, **2004**, *20*, 5809–5828; Tetracationic [2]catenanes, both degenerate and nondegenerate, have been studied as Langmuir films, by associating them with amphiphilic counterions. See: b) C. L. Brown, U. Jonas, J. A. Preece, H. Ringsdorf, M. Seitz, J. F. Stoddart, *Langmuir* **2000**, *16*, 1924–1930; c) M. Asakawa, M. Higuchi, G. Mattersteig, T. Nakamura, A. R. Pease, F. M. Raymo, T. Shimizu, J. F. Stoddart, *Adv. Mater.* **2000**, *12*, 1099–1102.

[10] For a discussion of first-principles computational methods which indicate that, when the $CBPQT^{4+}$ ring surrounds the DNP ring system, the switch is ON, whereas, when it surrounds the TTF unit, the switch is OFF, see: a) A. H. Flood, R. J. A. Ramirez, W.-Q. Deng, R. P. Muller, W. A. Goddard III, J. F. Stoddart, *Aust. J. Chem.* **2004**, *57*, 301–322; see also a report on "Computational Nanotechnology" by E. K. Wilson, *Chem. Eng. News* **2003**, April 28, 27–29; b) Y. H. Jang, S. Hwang, Y.-H. Kim, S. S. Jang, W. A. Goddard III, *J. Am. Chem. Soc.* **2004**, *126*, 12636–12645; c) W.-Q. Deng, R. P. Muller, W. A. Goddard III, *J. Am. Chem. Soc.* **2004**, *126*, 12636–12645.

[11] H.-R. Tseng, D. Wu, N. X. Fang, X. Zhang, J. F. Stoddart, *ChemPhysChem* **2004**, *5*, 111–116.

[12] a) D. G. Hamilton, J. E. Davies, L. Prodi, J. K. M. Sanders, *Chem. Eur. J.* **1998**, *4*, 608–620; b) A. C. Try, M. M. Harding, D. G. Hamilton, J. K. M. Sanders, *Chem. Commun.* **1998**, 723–724; c) D. G. Hamilton, J. K. M. Sanders, *Chem. Commun.* **1998**, 1749–1750; d) D. G. Hamilton, N. Feeder, L. Prodi, S. J. Test, W. Clegg, J. K. M. Sanders, *J. Am. Chem. Soc.* **1998**, *120*, 1096–1097; e) D. G. Hamilton, N. Feeder, S. J. Teat, J. K. M. Sanders, *New J. Chem.* **1998**, *22*, 1019–1021; f) D. G. Hamilton, L. Prodi, N. Feeder, J. K. M. Sanders, *J. Chem. Soc. Perkin Trans. 1* **1999**, 1057–1066; g) D. G. Hamilton, M. Montalti, L. Prodi, M. Fontai, P. Zanello, J. K. M. Sanders, *Chem. Eur. J.* **2000**, *6*, 608–617; h) J. G. Hansen, N. Feeder, D. G. Hamilton, M. J. Gunter, J. Becher, J. K. M. Sanders, *Org. Lett.* **2000**,

2, 449–452; i) M. J. Gunter, N. Bampos, K. D. Johnstone, J. K. M. Sanders, *New J. Chem.* **2001**, *25*, 166–173; j) K. D. Johnstone, N. Bampos, J. K. M. Sanders, M. J. Gunter, *Chem. Commun.* **2003**, 1396–1397.

[13] a) L. G. Schroff, A. J. A. van der Weerdt, D. H. J. Staalman, J. W. Verhoven, Th. J. de Boer, *Tetrahedron Lett.* **1973**, *14*, 1649–1652; b) D. G. Hamilton, D. E. Lynch, K. A. Byriel, C. H. L. Kennard, *Aust. J. Chem.* **1997**, *50*, 439–445.

[14] a) L. G. Schroff, R. L. Zsom, A. J. A. van der Weerdt, P. I. Schrier, J. P. Geert, N. M. M. Nibbering, J. W. Verhoeven, T. J. de Boer, *Recl. Trav. Chim. Pays-Bas* **1976**, *95*, 89–93; b) R. L. Zsom, L. G. Schroff, C. T. Bakker, J. W. Verhoeven, Th. J. de Boer, J. D. Wright, H. Kuroda, *Tetrahedron* **1978**, *34*, 3225–3232.

[15] G. Schill, K. Rissler, H. Fritz, W. Vetter, *Angew. Chem.* **1981**, *93*, 197–201; *Angew. Chem. Int. Ed. Engl.* **1981**, *20*, 187–189.

[16] The mono-electron reductions of a bare 1,4,5,8-naphthalenetetracarboxylic diimide (NpI) unit and a bare pyromellitic diimide (PmI) unit are known to be −700 mV and −950 mV, respectively. See: reference [12g].

[17] The clipping approach to rotaxane assembly relies on the macrocyclization of the subunits of a wheel-like component around the axle-like subunit of the dumbbell-shaped component. For recent examples, see: a) V. Balzani, A. Credi, S. J. Langford, L. Prodi, J. F. Stoddart, M. Venturi, *Supramol. Chem.* **2001**, *13*, 303–311; b) F. G. Gatti, D. A. Leigh, S. A. Nepogodiev, A. M. Z. Slawin, S. J. Teat, J. K. Y. Wong, *J. Am. Chem. Soc.* **2001**, *123*, 5983–5989; c) G. Doddi, G. Ercolani, S. Franconeri, P. Mencarelli, *J. Org. Chem.* **2001**, *66*, 4950–4953; e) D. A. Leigh, P. J. Lusby, S. J. Teat, A. J. Wilson, J. K. Y. Wong, *Angew. Chem.* **2001**, *113*, 1586–1591; *Angew. Chem. Int. Ed.* **2001**, *40*, 1538–1543; d) P. T. Glink, A. I. Oliva, J. F. Stoddart, A. J. P. White, D. J. Williams, *Angew. Chem.* **2001**, *113*, 1922–1927; *Angew. Chem. Int. Ed.* **2001**, *40*, 1870–1875; e) M. Horn, J. Ihringer, P. T. Glink, J. F. Stoddart, *Chem. Eur. J.* **2003**, *9*, 4046–4054; f) A. F. M. Kilbinger, S. J. Cantrill, A. W. Waltman, M. W. Day, R. H. Grubbs, *Angew. Chem.* **2003**, *115*, 3403–3407; *Angew. Chem. Int. Ed.* **2003**, *42*, 3281–3285.

[18] a) S. J. Rowan, S. J. Cantrill, G. R. L. Cousins, J. K. M. Sanders, J. F. Stoddart *Angew. Chem.* **2002**, *114*, 938–993; *Angew. Chem. Int. Ed.* **2002**, *41*, 898–952; b) R. L. E. Furlan, S. Otto, J. K. M. Sanders, *Proc. Natl. Acad. Sci. USA* **2002**, *99*, 4801–4804.

[19] The slippage methodology was exploited early on when rotaxanes were prepared in a statistical manner. For example see: a) I. T. Harrison, *J. Chem. Soc. Chem. Commun.* **1972**, 231–232; b) G. Schill, W. Beckmann, N. Schweikert, H. Fritz, *Chem. Ber.* **1986**, *119*, 2647–2655; the first successful template-directed synthesis of rotaxanes by the slippage approach was reported in 1993 see: c) P. R. Ashton; M. Belohradsky, D. Philp, J. F. Stoddart, *J. Chem. Soc. Chem. Commun.* **1993**, 1269–1274; for a discussion of the phenomenon see: d) M. C. T. Fyfe, F. M. Raymo, J. F. Stoddart, *Stimulating Concepts in Chemistry* (Eds.: M. Shibasaki, J. F. Stoddart, F. Vögtle), Wiley-VCH, Weinheim, **2000**, pp. 211–220; for recent examples see: e) Y. H. Sohgawa, H. Fujimori, J. Shoji, Y. Furusho, N. Kihara, T. Takata, *Chem. Lett.* **2001**, *8*, 774–775; f) J. O. Jeppesen, J. Becher, J. F. Stoddart, *Org. Lett.* **2002**, *4*, 557–560; g) A. M. Elizarov, T. Chang, S.-H. Chiu, J. F. Stoddart, *Org. Lett.* **2002**, *4*, 3565–3568; h) P. Linnartz, S. Bitter, C. A. Schalley, *Eur. J. Org. Chem.* **2003**, *24*, 4819–4829.

[20] P. R. Ashton, R. Ballardini, V. Balzani, M. Belohradsky, M. T. Gandolfi, D. Philp, L. Prodi, F. M. Raymo, M. V. Reddington, N. Spencer, J. F. Stoddart, M. Venturi, D. J. Williams, *J. Am. Chem. Soc.* **1996**, *118*, 4931–4951.

[21] M. Asakawa, P. R. Ashton, R. Ballardini, V. Balzani, M. Belohradsky, M. T. Gandolfi, O. Kocian, L. Prodi, F. M. Raymo, J. F. Stoddart, M. Venturi, *J. Am. Chem. Soc.* **1997**, *119*, 302–310.

[22] A. E. Martin, J. E. Bulkowski, *J. Org. Chem.* **1982**, *47*, 415–418.

[23] M. Asakawa, P. R. Ashton, S. E. Boyd, C. L. Brown, R. E. Gillard, O. Kocian, F. M. Raymo, J. F. Stoddart, M. S. Tolley, A. J. P. White, D. J. Williams, *J. Org. Chem.* **1997**, *62*, 26–37.

[24] C. Sotirious-Leventis, Z. Mao, *J. Heterocycl. Chem.* **2000**, *37*, 1665–1667.

[25] D. D. Perrin, W. L. F. Armarego, *Purification of Laboratory Chemicals*, Pergamon Press, New York, **1998**.

[26] a) P.-L. Anelli, N. Spencer, J. F. Stoddart, *J. Am. Chem. Soc.* **1991**, *113*, 5131–5133; b) P.-L. Anelli, M. Asakawa, P. R. Ashton, R. A. Bissell, G. Clavier, R. Gorski, A. E. Kaifer, S. J. Langford, G. Mattersteig, S. Menzer, D. Philp, A. M. Z. Slawin, N. Spencer, J. F. Stoddart, M. S. Tolley, D. J. Williams, *Chem. Eur. J.* **1997**, *3*, 1113–1135.

[27] Spinworks Version 2.1, K. Marat, Department of Chemistry, University of Manitoba (Canada).

[28] The rate of exchange was determined by using the separation between the peaks at low temperature (Figure 9d), $\Delta\nu = \sim 65$ Hz, and the equation for the rate of exchange at coalescence, $k_{ex} = (\pi\Delta\nu)/2$. This gives a value of $k_{ex} = 144\ s^{-1}$ at 239 K, from which the $\Delta G^{\ddagger}$ for this process can be calculated, and is determined to be ~11.5 kcal mol^{-1}. The numbers are the same for both **NpNpR** and **NpPmR** within experimental error.

[29] a) P. R. Ashton, S. E. Boyd, S. Menzer, D. Pasini, F. M. Raymo, N. Spencer, J. F. Stoddart, A. J. P. White, D. J. Williams, P. G. Wyatt, *Chem. Eur. J.* **1998**, *4*, 299–310; b) D. B. Amabilino, P. R. Ashton, J. A. Bravo, F. M. Raymo, J. F. Stoddart, A. J. P. White, D. J. Williams, *Eur. J. Org. Chem.* **1999**, 1295–1302; c) H.-R. Tseng, S. A. Vignon, P. C. Celestre, J. F. Stoddart, A. J. P. White, D. J. Williams, *Chem. Eur. J.* **2003**, *9*, 543–556.

[30] a) D. B. Amabilino, P.-L. Anelli, P. R. Ashton, G. R. Brown, E. Córdova, L. A. Godínez; W. Hayes, A. E. Kaifer, D. Philp, A. M. Z. Slawin, N. Spencer, J. F. Stoddart, M. S. Tolley, D. J. Williams, *J. Am. Chem. Soc.* **1995**, *117*, 11142–11170; b) J. A. Bravo, F. M. Raymo, J. F. Stoddart, A. J. P. White, D. J. Williams, *Eur. J. Org. Chem.* **1998**, 2565–2571; c) P. R. Ashton, J. A. Bravo, F. M. Raymo, J. F. Stoddart, A. J. P. White, D. J. Williams, *Eur. J. Org. Chem.* **1999**, 899–908.

[31] For MeCN solution see: P. R. Ashton, R. Ballardini, V. Balzani, A. Credi, M. T. Gandolfi, S. Menzer, L. Pérez-García, L. Prodi, J. F. Stoddart, M. Venturi, A. J. P. White, D. J. Williams, *J. Am. Chem. Soc.* **1995**, *117*, 11171–11197.

[32] T. C. Barrows, S. Brochsztain, V. G. Toscano, P. B. Filho, M. J. Politi, *J. Photochem. Photobiol. A* **1997**, *111*, 97–104.

[33] a) R. Ballardini, M. T. Gandolfi, V. Balzani, in *Electron Transfer in Chemistry*, *Vol. 3* (Ed.: V. Balzani), Wiley-VCH, Weinheim, **2001**, pp. 539–581; b) R. Ballardini, V. Balzani, A. Credi, M. T. Gandolfi, M. Venturi, *Acc. Chem. Res.* **2001**, *34*, 445–455.

[34] A. Viehbeck, M. J. Goldberg, C. A. Kovac, *J. Electrochem. Soc.* **1990**, *137*, 1460–1466.

[35] a) C. M. Cordova, S. Mendoza, A. E. Kaifer, *Chem. Soc. Rev.* **2000**, *29*, 37–42; b) C. B. Gorman, J. C. Smith, *Acc. Chem. Res.* **2001**, *34*, 60–71.

[36] G. Kaiser, T. Jarrosson, S. Otto, Y.-F. Ng, A. D. Bond, J. K. M. Sanders, *Angew. Chem.* **2004**, *116*, 1993–1996; *Angew. Chem. Int. Ed.* **2004**, *43*, 1959–1962.

[37] S. A. Vignon, T. Jarrosson, T. Iijima, H.-R. Tseng, J. K. M. Sanders, J. F. Stoddart, *J. Am. Chem. Soc.* **2004**, *126*, 9884–9885.

[38] The K_a value for binding of $LiClO_4$ by [12]crown-4 at 298 K in acetonitrile solution is $2042\ M^{-1}$; see A. F. Danil de Namor, J. C. Y. Ng, M. A. L. Tanco, M. Saloman, *J. Phys. Chem.* **1996**, *100*, 14485–14491.

[39] a) S. Y. Chia, J. G. Cao, J. F. Stoddart, J. I. Zink, *Angew. Chem.* **2001**, *113*, 2513–2517; *Angew. Chem. Int. Ed.* **2001**, *40*, 2447–2451; b) K. Kim, W. S. Jeon, J.-K. Kang, J. W. Lee, S. Y. Jon, Y. Kim, K. Kim *Angew. Chem.* **2003**, *115*, 2395–2398; *Angew. Chem. Int. Ed.* **2003**, *42*, 2293–2296; c) R. Hernandez, H.-R. Tseng, J. W. Wong, J. F. Stoddart, J. I. Zink *J. Am. Chem. Soc.* **2004**, *126*, 3370–3371; d) E. Katz, L. Sheeney-Haj-Ichia, I. Willner, *Angew. Chem.* **2004**, *116*, 3354–3362; *Angew. Chem. Int. Ed.* **2004**, *43*, 3292–3300.

[40] J. D. Badjic, V. Balzani, A. Credi, S. Silvi, J. F. Stoddart, *Science* **2004**, *303*, 1845–1849.

[41] I. B. Berlman, *Handbook of Fluorescence Spectra of Aromatic Molecules*, Academic Press, London, **1965**.

[42] D. Dubois, G. Mininot, W. Kutner, M. T. Jones, K. M. Kadish, *J. Phys. Chem.* **1992**, *96*, 7137–7145.

[43] J. B. Flanagan, S. Margel, A. J. Bard, F. C. Anson, *J. Am. Chem. Soc.* **1978**, *100*, 4248–4253.

[44] DigiSim 3.05, BioAnalytical Systems, West Lafayette, IN; www.bioanalytical.com.

Received: June 28, 2004
Published online: November 5, 2004

